# Adaptive short-term plasticity in the typical reading network

S. Turker [a,b,*,+], P. Kuhnke [a,b,+], F.R. Schmid [c], V.K.M. Cheung [d], K. Weise [e], M. Knoke [a], B. Zeidler [f], K. Seidel [a], L. Eckert [a], G. Hartwigsen [a,b]

[a] *Lise Meitner Research Group Cognition and Plasticity, Max Planck Institute for Human Cognitive and Brain Sciences, Stephanstr. 1a, Leipzig 04103, Germany*
[b] *Wilhelm Wundt Institute for Psychology, University of Leipzig, Germany*
[c] *CBC Center for Brain and Cognition, Universitat Pompeu Fabra, Barcelona, Spain*
[d] *Institute of Information Science, Academia Sinica, Taipei, Taiwan*
[e] *Methods and Development Group Brain Networks, Max Planck Institute for Human Cognitive and Brain Sciences, Leipzig, Germany*
[f] *Centre for Systematic Musicology, University of Graz, Austria*

## ARTICLE INFO

## ABSTRACT

The left temporo-parietal cortex (TPC) is crucial for phonological decoding, i.e., for learning and retaining sound-letter mappings, and appears hypoactive in dyslexia. Here, we tested the causal contribution of this area for reading in typical readers with transcranial magnetic stimulation (TMS) and explored the reading network's response with fMRI. By investigating the underlying neural correlates of stimulation-induced modulations of the reading network, we can help improve targeted interventions for individuals with dyslexia. 28 typical adult readers overtly read simple and complex words and pseudowords during fMRI after effective and sham TMS over the left TPC. To explore differences in functional activation and effective connectivity within the reading network, we performed univariate and multivariate analyses, as well as dynamic causal modeling. While TMS-induced effects on reading performance and brain activation showed large individual variability, multivariate analyses revealed a shift in activation in the left inferior frontal cortex for pseudoword reading after effective TMS. Furthermore, TMS increased effective connectivity from the left ventral occipito-temporal cortex to the left TPC. In the absence of effects on reading performance, the observed changes in task-related activity and the increase in functional coupling between the two core reading nodes suggest successful short-term compensatory reorganization in the reading network following TMS-induced disruption. This study is the first to explore neurophysiological changes induced by TMS to a core reading node in typical readers while performing an overt reading task. We provide evidence for remote stimulation effects and emphasize the relevance of functional interactions in the reading network.

## 1. Introduction

The ability to process written language is crucial for everyday life, work, and interpersonal communication and can thus be seen as a core feature of human communication. However, fluent reading requires years of instruction and practice, and is based upon multiple, hierarchically organized processes, including orthographic recognition, orthographic-phonological mapping, and semantic access (Xia et al., 2018). In adults, known words are usually directly accessed as whole forms in the mental lexicon (so-called sight word reading), while meaningless pseudowords require phonological decoding, i.e., grapheme-phoneme conversion (Coltheart et al., 2001; Ehri, 2005). At

the neural level, coordinating these various processes relies largely upon three brain regions that are classically associated with language processing: (i) the left inferior frontal gyrus (IFG), (ii) the left temporo-parietal cortex (TPC) and (iii) the left ventral occipito-temporal cortex (vOTC) (Pugh et al., 2001; Rueckl et al., 2015). While the left IFG is engaged in processes of attention and language (e.g., phonological output resolution; Taylor et al., 2013), the left TPC is responsible for the transformation of orthographic elements into associated phonological codes (Linkersdörfer et al., 2012). Evidence for the crucial role of the left TPC also comes from dyslexia research, showing that this region is significantly hypoactive in individuals with dyslexia across all age groups (Richlan et al., 2011; Turker, 2018). The last region, the left

vOTC, gradually develops sensitivity to print (Chyl et al., 2021) and optimizes linguistic processing for quick access to familiar words (Gagl et al., 2020). It also contains the so-called visual word form area, which develops during reading acquisition (Dehaene & Cohen, 2011).

Although non-invasive brain stimulation (NIBS) studies have proliferated over the past decades, few studies have applied NIBS to specifically modulate reading processing (Turker & Hartwigsen, 2021). Existing NIBS studies with typical readers provide first evidence that the left IFG contributes to phonological and semantic reading-related processes (e.g., Devlin et al., 2003; Gough et al., 2005; Hartwigsen, Baumgaertner, et al., 2010; Hartwigsen, Price, et al., 2010), while the left vOTC is critical for word and pseudoword processing (Duncan et al., 2010; Pattamadilok et al., 2015). Moreover, the left TPC was found to be important for phonological processes related to reading, in line with its expected role as grapheme-phoneme-conversion center (Costanzo et al., 2012a; Liederman et al., 2003).

Likewise, NIBS studies with atypical readers also suggest that single- and multiple-session interventions targeting the left and right TPC can improve reading performance in children and adults with dyslexia (Costanzo et al., 2013, 2019; Lazzaro et al., 2021; see review by Turker & Hartwigsen, 2022). However, existing NIBS studies did not combine stimulation with neuroimaging, leaving the underlying neural correlates of stimulation-induced modulations of the reading network unclear. The observed behavioural modulations most likely stem from (1) an in- or decrease in functional brain activation in the targeted area (Miniussi et al., 2013), (2) up- and down-regulations of tightly connected brain regions or regions within the same network (Sale et al., 2015), and (3) changes in functional connectivity between network nodes (e.g., successful reading relies upon functional connectivity within the reading network; Schurz et al., 2015; van der Mark et al., 2011). Such compensatory short-term mechanisms occur after disruption of an area and may be correlated with changes in behavioural performance (Hartwigsen et al., 2013; Hartwigsen, Henseler, et al., 2017).

In the present study, we investigated if inhibition of the left TPC impacts word and pseudoword processing in typical adult readers to shed light on the causal role of this area for different reading processes, and explored the reading network's response to perturbation in terms of functional activation and connectivity. We hypothesized that an inhibition of the left TPC would lead to (1) increased reading times (speech onsets) and decreased accuracy for simple and complex pseudowords, (2) an up-regulation of the left IFG, vOTC and the contralateral right TPC and (3) higher functional coupling with the disrupted region. To test these hypotheses, we applied offline effective and sham repetitive transcranial magnetic stimulation (rTMS) to the left TPC of healthy adults with no dyslexia history who then performed an overt reading task during functional MRI (see Fig. 1). We believe that this approach
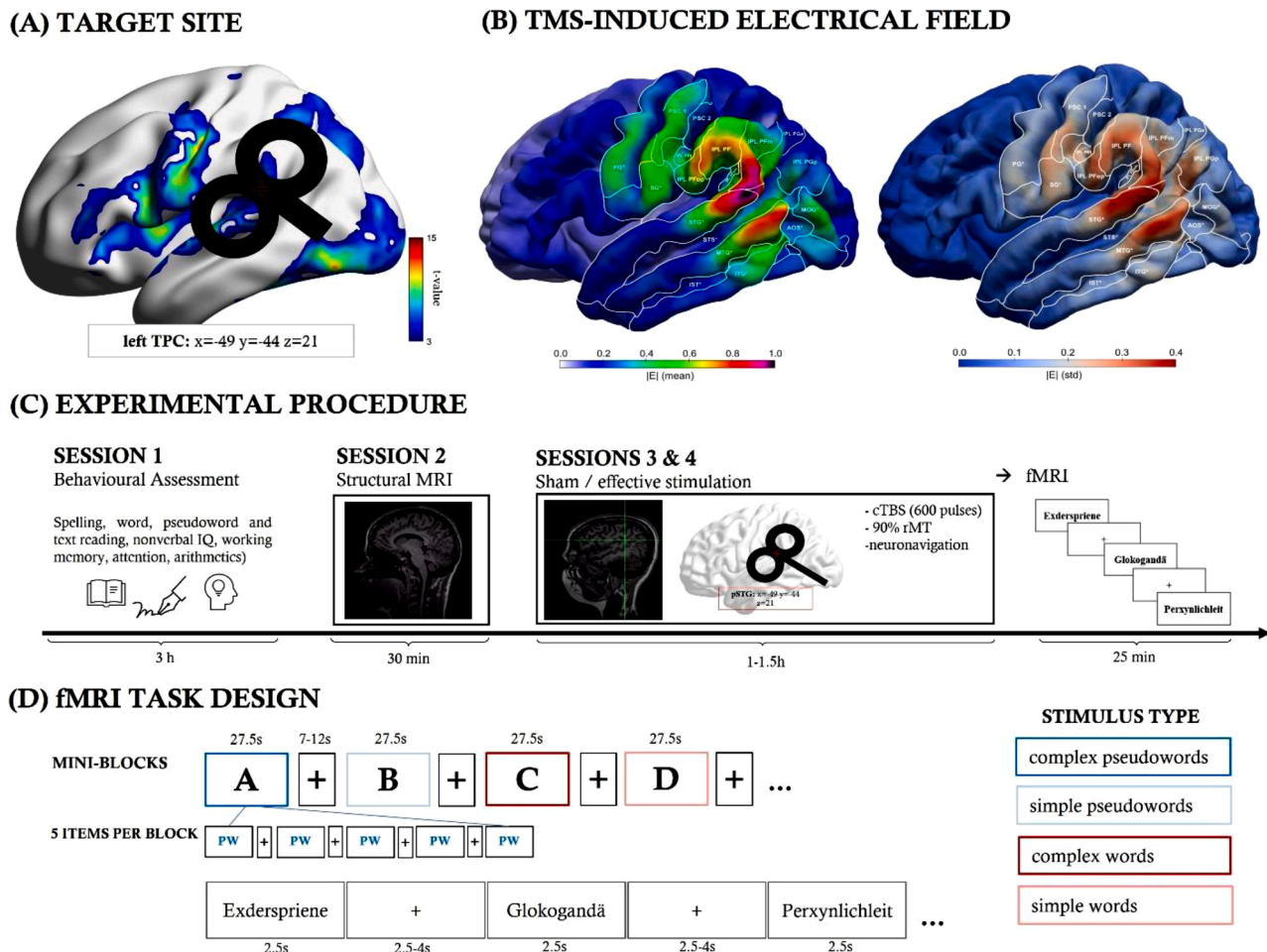


**Fig. 1.** *Experimental design.* (A) The TMS-target in the left TPC was chosen based on previous meta-analyses (MNI coordinates: x/y/z= -49/-44/21) and is displayed on the averaged functional activation map for the contrast [all trials > rest] of the sham session in the present study. (B) Electrical field simulations show both the mean induced electrical field (V/m) and the standard deviation across participants during left TPC stimulation. (C) In the first session, behavioural assessment took place. In the second session, we collected structural scans for neuronavigation during sessions 2 and 3, in which effective and sham continuous theta burst stimulation (cTBS) at 90% of the resting motor threshold (rMT) was applied over the target region. (D) During fMRI, subjects overtly read visually presented simple and complex words and pseudowords in mini-blocks (five items per block) displayed for 2.5 seconds in the scanner (200 trials per scanning session spread over the four conditions; total duration: ~25 minutes). We jittered the inter-stimulus interval (2.5–4 seconds) and rest during mini-blocks (7–12 seconds).

can help us advance our knowledge on reading and help explore the potential of neuromodulatory interventions for individuals with reading impairments.

## 2. Materials and methods

### 2.1. Participants

Participants were young, healthy, right-handed adults (N = 28; 13 females; range: 18–40 years, $M_{age} = 25 \pm 4$) with no prior history of psychiatric, neurological, hearing, or developmental disorders. All participants had nonverbal intelligence scores within the normal range or above (nonverbal IQ: $\geq$ 91; CFT 20-R; Weiß, 2019). Sample size was determined based on comparable previous TMS studies (e.g., Kuhnke et al., 2020) and sensitivity analyses were performed to confirm the chosen sample size was sensitive enough to detect the expected effect sizes (see Section 2.4.2). Participants were either recruited via the participants database of the Max Planck Institute for Human Cognitive and Brain Sciences Leipzig (MPI CBS), or flyers, posters, and social media. Participation in all sessions was required for the respective participant's data to be included in the study sample. Prior to participation, written informed consent was obtained from each subject. The study was performed according to the guidelines of the Declaration of Helsinki and approved by the local ethics committee of the University of Leipzig.

### 2.2. Experimental design

The present offline TMS-fMRI study comprised a behavioural testing session, a structural MRI session and two sessions of TMS (effective and sham stimulation) followed by fMRI. During the separate behavioural testing session, we assessed nonverbal intelligence, working memory, reading and spelling for a later comparison of these skills with a group of individuals with dyslexia. Please note that the present analyses comprise only the study with the healthy, typical adult readers. The TMS-fMRI sessions were separated by at least 7 days to prevent carry-over effects of TMS, and session order (sham or effective) was counterbalanced across participants with a few exceptions. The study employed a 2×2×2 within-subject design with the factors TMS (effective stimulation, sham stimulation), stimulus type (words, pseudowords) and complexity (simple stimuli consisting of two syllables and 4–6 letters, complex stimuli consisting of three to four syllables and 10-14 letters) (for details of the experimental procedure, stimulation site and fMRI design, see Fig. 1).

#### 2.2.1. Behavioural testing

Since the present study was part of a larger project which further aimed to compare individuals with and without dyslexia, the present group of typical readers underwent a 3-hour behavioural testing session that included various measures of reading (word, nonword and text reading) (Moll & Landerl, 2010; Schneider et al., 2017), spelling (Kersting & Althoff, 2003) and general cognitive testing [e.g., working memory (Wechsler, 2008)]. To rule out arithmetic difficulties (i.e., dyscalculia), attention deficits (e.g., attention deficits hyperactivity disorder) and low intelligence in the present sample, we further assessed arithmetic competence, continuous attention and nonverbal IQ (Holzer et al., 2017; Knye et al., 2003; Weiß, 2019). For the present sample, no subject had to be excluded and none met the criteria for reading and spelling difficulties, which were set at 1.5 standard deviations below the group mean in at least 50% of administered reading and spelling tests.

#### 2.2.2. Stimuli

We used an event-related mini-block design that used 400 stimuli altogether (200 simple and complex words; 200 simple and complex pseudowords). In each session, participants overtly read a random compilation of 100 words (50 simple, 50 complex) and 100 pseudowords (50 simple, 50 complex) in mini-blocks of 5 stimuli in the scanner.

Note that no stimulus was repeated across sessions to avoid learning effects. The 200 simple word stimuli consisted of two syllables and 4–6 letters and were the same as used in Schuster et al. (2015). As complex words, we chose the first 100 most frequent 4-syllabic words (10–14 letters) from the dlex database (http://www.dlexdb.de/). We first excluded compound words and plurals but due to the small number of available complex words we had to include several 3-syllabic words and plurals with 10–14 letters. Pseudowords were then designed using Wuggy (http://crr.ugent.be/programs-data/wuggy) based on the simple and complex word lists. To make sure none of the observed effects were due to differences in orthographic neighbourhood or lexical frequency of items, we included orthographic neighborhood (orthographic Levenshtein distance 20) and lexical frequency for all items (set at 0 for all pseudowords) as covariates in statistical analyses.

#### 2.2.3. Functional neuroimaging

Functional MRI data were collected on a 3T Siemens Magnetom Skyra scanner (Siemens, Erlangen, Germany) with a 32-channel head coil. Blood oxygenation level-dependent (BOLD) images were acquired with a single-echo BOLD EPI sequence (repetition time [TR]: 2 s; echo time [TE]: 22 ms; flip angle: 80°; field of view [FoV]: 204 mm; voxel size: 2.5 × 2.5 × 2.5 mm; bandwidth: 1794 Hz/Px; phase encoding direction: A/P; multiband acceleration factor: 3). B0 field maps were acquired for susceptibility distortion correction using a spin-echo EPI sequence (TR: 8000 ms; TE:50 ms; flip angle: 90°; bandwidth: 1794 Hz/Px; other parameters identical to functional sequence).

During fMRI, stimuli were presented for 2.5 seconds. We jittered the between-stimulus-interval (2.5–4 s), as well as the between-mini-block-interval (7–12 s; see Fig. 1). Subjects were instructed to read out all stimuli as fast and correctly as they could with as little head movement as possible. Subjects' in-scanner responses were recorded and manually preprocessed with Audacity (Audacity Team, 2021) to remove scanner noise. Speech on- and offsets were determined with Praat (Boersma & Weening, 2021) by four independent raters, two analyzing each audio-file in 50% of cases. We computed an interrater reliability >0.85, suggesting high reliability among raters. For the following analyses, we averaged speech onsets across raters if they were rated by more than one person. Accuracy for all trials was checked by a third person.

### 2.3. Transcranial magnetic stimulation (TMS)

To investigate the causal role of the left TPC for phonological processing, we applied offline continuous theta burst stimulation (cTBS). cTBS applies bursts of 3 stimuli at 50 Hz repeated at intervals of 200 ms (5 Hz) for 40 seconds (total: 600 pulses) (Huang et al., 2005). Biphasic TMS pulses were applied via a MagPro X100 stimulator (MagVenture, Farum, Denmark) equipped with a passively cooled MCF-B65 figure-e-of-eight coil. Offline protocols can induce adaptive changes in brain activity and connectivity that outlast the stimulation for up to 60 minutes (Siebner & Rothwell, 2003). Participants underwent one effective and one sham (placebo) session. The sham condition mirrored the effective condition in terms of basic set-up and procedure, but a placebo coil (MCF-P-B65) was used, which features the same mechanical outline and acoustic noise as the effective coil but reduces the magnetic field strength by ~80%. Intensity of the stimulation was set at 90% of the individual resting motor threshold (rMT). The protocol for assessing the resting motor threshold was conducted in accordance with a standardized procedure (Schutter & van Honk, 2006).

The MNI coordinates for the left TPC (x = -49, y = -44, z = 21) were calculated from three meta-analyses on reading impairments (Maisog et al., 2008; Richlan et al., 2009, 2011). To precisely target these coordinates in each individual participant, they were transformed from MNI to subject space using the SPM12 software (Wellcome Trust Center for Neuroimaging, University College London, UK). We then used stereotactic neuronavigation (TMS Navigator, Localite GmbH, Sankt Augustin, Germany) to navigate the coil over the target area and

maintain its location throughout stimulation. For neuronavigation, participants' heads were co-registered onto their T1-weighted MR image before the stimulation sessions. T1 scans had been obtained beforehand with a 3T MRI scanner (Siemens, Erlangen, Germany) using an MPRAGE sequence (176 slices in sagittal orientation; repetition time: 2.3 s; echo time: 2.98 ms; field of view: 256 mm; voxel size: $1{\times}1{\times}1$ mm; no slice gap; flip angle: $9°$; phase encoding direction: A/P).

### 2.4. Data analysis

#### 2.4.1. Data and code availability

All data and code is available at the following OSF registry: osf.io/fpgcy (Turker & Kuhnke, 2023).

#### 2.4.2. Behavioural analyses

Behavioural data from in-scanner performance of one participant were not usable due to technical problems with the speech recording software, leaving a total of 27 subjects for behavioural analyses. Speech onsets and response accuracy of each trial were analysed with generalised linear mixed models (GLMM) using glmmTMB 1.1.2.3 (Brooks et al., 2017) in R 4.0.5 (R Core Team, 2022). To circumvent the need to transform reaction times to satisfy normality assumptions, reading times were modelled using a Gamma distribution with the identity link function (Lo & Andrews, 2015). The accuracy of each trial (correct versus incorrect) was modelled as a binary response using a binomial distribution and logit link function. All models included as fixed effects the four-way interaction between TMS (effective vs. sham), stimulus type (word vs. pseudoword), complexity (simple vs. complex) and session (effective in first vs. effective in second session) and all lower order terms. A maximal random effects structure was used for all models with subject as the grouping variable to avoid inflated Type I errors (Barr et al., 2013). The resulting GLMM for speech onsets included random intercepts and random slopes for the interaction between TMS, stimulus type and complexity, as well as all lower order terms. Likewise, random intercepts and random slopes for TMS and complexity were included in the GLMM for response accuracy. For each item, orthographic neighbourhood (OLD20) and lexical frequency (lexfreq) were calculated and added as covariates in the models. The significance of each variable was assessed using the Wald test, and marginal effects were calculated using a step-down simple effects analysis.

Earlier TMS studies that aimed to modulate reading performance had reported strong TMS effects with Cohen's *d* ranging from -0.37 to 1.96 based on repeated measures ANOVAs with ten subjects (Costanzo et al., 2012b, 2013). Similarly, work from our own group revealed strong TMS effects after left TPC stimulation in a group of 26 subjects (Cohen's $d = 0.63$) (Kuhnke, Beaupain, et al., 2020). We used G-power to perform a sensitivity calculation, which reveals the smallest effect that could have been detected with high probability given our sample size. The sensitivity analysis showed that assuming $\alpha = 0.05$, we had 80% power to detect effect sizes larger than 0.55 (Cohen's *dz*) for two-tailed *t*-tests and larger than 0.46 (Cohen's *d*) for repeated measures ANOVAs (Faul et al., 2007).

#### 2.4.3. fMRI analysis

Preprocessing was performed using *fMRIprep* (version 20.2.1; Esteban et al. 2019) and univariate analyses were performed using the two-level approach in *SPM12*. A multivariate pattern analysis (MVPA) was performed with *The Decoding Toolbox* (Hebart et al., 2015), and effective connectivity within the reading network was measured with *Dynamic Causal Modeling* (DCM) (Friston et al., 2003).

##### 2.4.3.1. Univariate analyses. We performed a whole-brain random-effects group analysis based on the general linear model (GLM), using the two-level approach in *SPM12*. First, individual participant data were modeled separately. The participant-level GLM included regressors for the four experimental conditions (simple words, complex words, simple pseudowords, complex pseudowords), modeling trials as box car functions (2.5 seconds duration) convolved with the canonical hemodynamic response function (HRF). Only correct trials with given responses (incorrect trials were trials without response or with completely wrong words/ pseudowords) were analyzed, error trials were modeled in a separate regressor-of-no-interest. To control for movement artifacts, we included the motion parameters from realignment into the subject-level GLM. To further improve motion confound regression, we also added the motion parameters' temporal derivatives, quadratic terms, and temporal derivatives of the quadratic terms. Therefore, nuisance regressors included 24 motion regressors (i.e., the 6 base motion parameters + 6 temporal derivatives of the motion parameters + 12 quadratic terms of the motion parameters and their temporal derivatives) (Friston et al., 1996; Satterthwaite et al., 2013). Moreover, we performed "motion scrubbing" to remove individual time points with strong volume-to-volume movement from the analysis (Power et al., 2012) . To this end, we computed framewise displacement (FD) as a measure of excessive volume-to-volume movement and added individual regressors for volumes that exceeded a threshold of FD > 0.9, as proposed for task-based fMRI data (Siegel et al., 2014). Finally, we included the top 10 aCompCor regressors explaining the most variance in physiological noise (Behzadi et al., 2007). The data were subjected to an AR(1) auto-correlation model to account for temporal auto-correlations, and high-pass filtered (cutoff 128 s) to remove low-frequency noise.

Contrast images for each participant were computed at the first level. At the second level, these contrast images were submitted to one-sample or paired *t*-tests (to test for interactions). For all second-level analyses, a gray matter mask was applied, restricting statistical tests to voxels with a gray matter probability > 0.1 (MNI152NLin2009cAsym gray matter template in *fMRIprep*). All activation maps were thresholded at a voxel-wise $p < .001$ and a cluster-wise $p < .05$ FWE-corrected.

##### 2.4.3.2. Multivariate analysis. As univariate analyses are insensitive to information represented in fine-grained, multi-voxel activation patterns (Haxby et al., 2014), we additionally performed a multivariate pattern analysis (MVPA) using *The Decoding Toolbox* (version 3.999F; Hebart et al., 2015) implemented in *Matlab* (version 2021a). Our MVPA aimed to test whether effective TMS over left TPC, as compared to sham TMS, modulated activity patterns in the stimulated or other, remote brain regions. We employed a searchlight MVPA, moving a spherical region-of-interest (or "searchlight") of 5 mm radius through the entire brain (Kriegeskorte et al., 2006). At each searchlight location, a machine-learning classifier (an L2-norm support vector machine; C=1) aimed to decode between effective and sham TMS, separately for words and pseudowords. We used leave-one-*participant*-out cross validation (CV), training on the activation patterns from n-1 participants and testing on the left-out participant (yielding 28 CV-folds). For statistical inference, we performed a permutation test across the accuracy-minus-chance maps of the different CV-folds (using *SnPM13 by Nichols, 2023*; as proposed by Wang et al., 2021), thresholded at a voxel-wise $p < .001$ and a cluster-wise $p < .05$ FWE-corrected (as in our univariate analyses). Activity patterns comprised beta estimates for each mini-block of every participant.

##### 2.4.3.3. Dynamic causal modeling (DCM). We performed DCM (Friston et al., 2003) to investigate TMS-induced changes in effective connectivity (i.e., directed causal influences) between the core nodes of the reading network. DCM estimates a model of effective connectivity between brain regions to predict a neuroimaging time series. A DCM consists of three types of parameters: 1) "intrinsic" (i.e., condition-independent) directed connections between brain regions, 2) "modulatory inputs" that change connection strengths during a certain experimental manipulation, and 3) "driving inputs" that drive activity in the network. The goal of DCM is to optimize a tradeoff between model fit

(of the predicted to observed time series) and complexity (i.e., deviation of model parameters from their prior expectations), measured by the model evidence (Kahan & Foltynie, 2013; Zeidman, Jafarian, Corbin, et al., 2019).

We performed a two-level analysis using Parametric Empirical Bayes (PEB) and Bayesian Model Reduction (BMR)—the current gold standard (Friston et al., 2016). At the first level, a "full model" was specified and estimated for each participant. Regions included in the model were the left TPC (the stimulated region), left vOTC, and left IFG. The three regions were defined functionally in each individual participant as the top 10% most activated voxels for [all sham trials > rest] within 20 mm spheres around the MNI peak coordinates in a meta-analysis of reading in adults (Martin et al., 2016): left TPC = -49/-44/21; left IFG = -52/20/18; left vOTC = -42/-68/-22. All regions were restricted to the cerebral gray matter. The first eigenvariate of the BOLD time series of each region was extracted and adjusted for effects-of-interest (all experimental conditions) using our participant-level GLM (see Univariate analyses). DCM inputs were mean-centered, so that the intrinsic connections reflected the mean connectivity across experimental conditions (Zeidman, Jafarian, Corbin, et al., 2019).

At the second level, DCM parameters of individual participants were entered into a GLM—the PEB model—that decomposed interindividual variability in connection strengths into group effects and random effects. BMR then compared the full model against numerous reduced models that had certain parameters "switched off" (i.e., prior mean and variance set to 0) (Friston et al., 2016). Finally, we computed the Bayesian model average (BMA), the average of parameter values across models weighted by each model's posterior probability (Pp) (Penny et al., 2007). This approach is preferred over exclusively assessing the parameters of the "best" model as it accommodates uncertainty about the true underlying model (Friston et al., 2016). The BMA was thresholded to only retain parameters with a Pp > 99%. For each modulatory input, we calculated the resulting connectivity value (in Hz) using formula 3 in Zeidman, Jafarian, Seghier, et al. (2019). Finally, to determine whether one experimental condition modulated a certain connection more strongly than another, we directly compared different parameters on the same connection using Bayesian contrasts (cf. Kuhnke et al., 2021).

## 3. Results

### 3.1. Functional activation results

Neuroimaging results of the sham session showed that word and pseudoword reading engaged distributed but also overlapping areas, including the target site in the left TPC (see Figure S1 for details of both conditions > rest). Yet, the direct comparison of both conditions revealed distinct activation patterns for pseudowords and words, especially within the left TPC. Overall, words showed a greater recruitment of regions of the default mode network (Smallwood et al., 2021), e.g., the bilateral angular gyri, middle temporal gyri, middle frontal cortices, and bilateral medial prefrontal and posteromedial cortices (Fig. 2A). Pseudowords, in contrast, activated classical reading areas, such as the bilateral vOTC and portions of the inferior parietal lobe and IFG more strongly (Fig. 2B). Whereas the left TPC activation for words covered mainly the angular gyrus, pseudowords recruited more posterior regions in the supramarginal gyrus (SMG), extending to the superior parietal lobe (SPL).

In terms of cerebellar engagement, we found robust word- and pseudoword-specific patterns of activation in the present study. Pseudoword reading when compared to word reading involved a large cluster spreading across lobules VIIIa / VIIb / VI and crus II in the right cerebellum, and a small cluster occupying specifically portions of lobules VIIIa / VIIIb in the left cerebellum. Word reading, in contrast, recruited primarily crus I and II in the left and right cerebellum.

To test for stimulus-specific recruitment in the left TPC region, we investigated activation magnitude in five designated ROIs that had been differentially engaged in the word vs. pseudoword contrasts (see Fig. 2). We included left angular gyrus (AG), left pSTG, left posterior SMG (pSMG), left anterior SMG (aSMG) and left SPL based on the Harvard-Oxford atlas in FSL (Desikan et al., 2006; Frazier et al., 2005; Goldstein et al., 2007; Makris
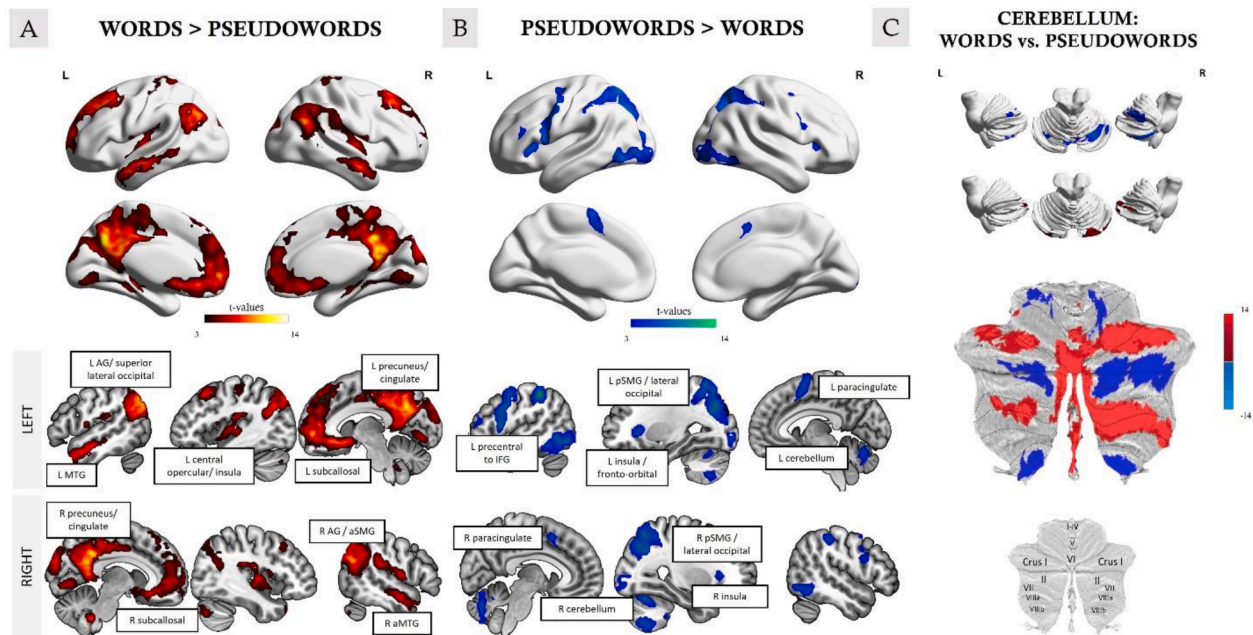


**Fig. 2.** *Cortical and cerebellar findings for the univariate contrasts for word vs. pseudoword reading during the sham (i.e., placebo) session.* All results are corrected at $p <$ .001 voxel-level and FWE-cluster-corrected at $p < .05$. (A) Brain areas displaying higher activation for words than pseudowords (red). Sagittal slices (x = ± 10 / ± 30 / ± 58) were chosen to display all significant clusters for words: bilateral subcallosal, bilateral AG, bilateral aMTG, bilateral precuneus / cingulate, left insula / central opercular cortex. (B) Regions displaying higher activation for pseudowords than words (blue). Sagittal slices (x = ± 6 / ± 28 / ± 50) further display all significant clusters: bilateral cingulate, bilateral cerebellum, bilateral insula /fronto-orbital cortex, bilateral lateral occipital cortex and left precentral gyrus to IFG. (C) Cerebellar activation for words > pseudowords (red) and pseudowords > words (blue), shown on a smoothed reconstruction (top) and a cerebellar flatmap.

et al., 2006). Repeated measures ANOVAs revealed main effects for stimulus type in left AG ($F_{(27,1)} = 61.5$, $p < .001$, Cohen's $d = 1.53$), left aSMG ($F_{(27,1)} = 21.9$, $p < .001$, Cohen's $d = 1.22$), left pSTG ($F_{(27,1)} = 6.3$, $p = .02$, Cohen's $d = 0.63$) and left SPL ($F_{(27,1)} = 42.2$, $p < .001$, Cohen's $d = 1.37$). Whereas left AG showed significantly less activation in the form of deactivation for pseudowords, the other three regions showed higher activation for pseudowords than words (Fig. 3). In addition to stimulus-type-effects, we also found significant complexity effects for left AG ($F_{(27,1)} = 28.4$, $p < .001$, Cohen's $d = 0.84$), left pSTG ($F_{(27,1)} = 12.2$, $p = .002$, Cohen's $d = 0.77$) and left SPL ($F_{(27,1)} = 5.6$, $p = .03$, Cohen's $d = 0.46$). The interaction between word type and complexity was further significant for left AG ($F_{(27,1)} = 4.9$, $p = .04$, Cohen's $d = 0.35$), with significant differences between simple words and simple pseudowords ($t = 4.2$, $p < .001$, Cohen's $d = 0.67$), simple words and complex pseudowords ($t = 9.4$, $p < .001$, Cohen's $d = 1.49$), simple and complex pseudowords ($t = 5.32$, $p < .001$, Cohen's $d = 0.82$) and complex words and pseudowords ($t = 7.22$, $p < .001$, Cohen's $d = 1.15$) as revealed by post hoc-tests (Holm-corrected).

Regarding functional activation for complexity, we found higher activation for complex stimuli in the bilateral motor cortices, the bilateral STG and areas within the posterior parietal cortex and occipital lobes (Fig. 4A). The same areas were more engaged during pseudoword as compared to word processing, suggesting that pseudoword activation patterns resembled complex item patterns due to higher cognitive demand. Likewise, simple items displayed a more word-like activation (Fig. 4B). As mentioned before, ROI analyses revealed effects for complexity in left AG ($F_{(27,1)} = 28.4$, $p < .001$, Cohen's $d = 0.84$), left pSTG ($F_{(27,1)} = 12.2$, $p = .002$, Cohen's $d = 0.77$) and left SPL ($F_{(27,1)} = 5.6$, $p = .03$, Cohen's $d = 0.46$), suggesting that the left SPL and left pSTG are specifically recruited during more complex reading tasks.

### 3.2. TMS effects on reading performance

We found that regardless of TMS condition, participants showed significantly longer speech onset times for pseudowords as compared to words ($z = 7.39$, $p < .001$) and for complex as compared to simple stimuli ($z = 3.072$, $p = .002$). Also, the interaction between the two was significant ($z = 7.744$, $p < .001$). Post-hoc tests revealed that all comparisons were significant: simple vs. complex words ($t = -3.737$, $p = .0002$), simple vs. complex pseudowords ($t = -11.612$, $p < .0001$), simple words vs. simple pseudowords ($t = -8.820$, $p < .0001$) and complex words vs. complex pseudowords ($t = -17.478$, $p < 0.0001$) (see Tables S1-S3 for details). Regarding reading times, we also found significant main
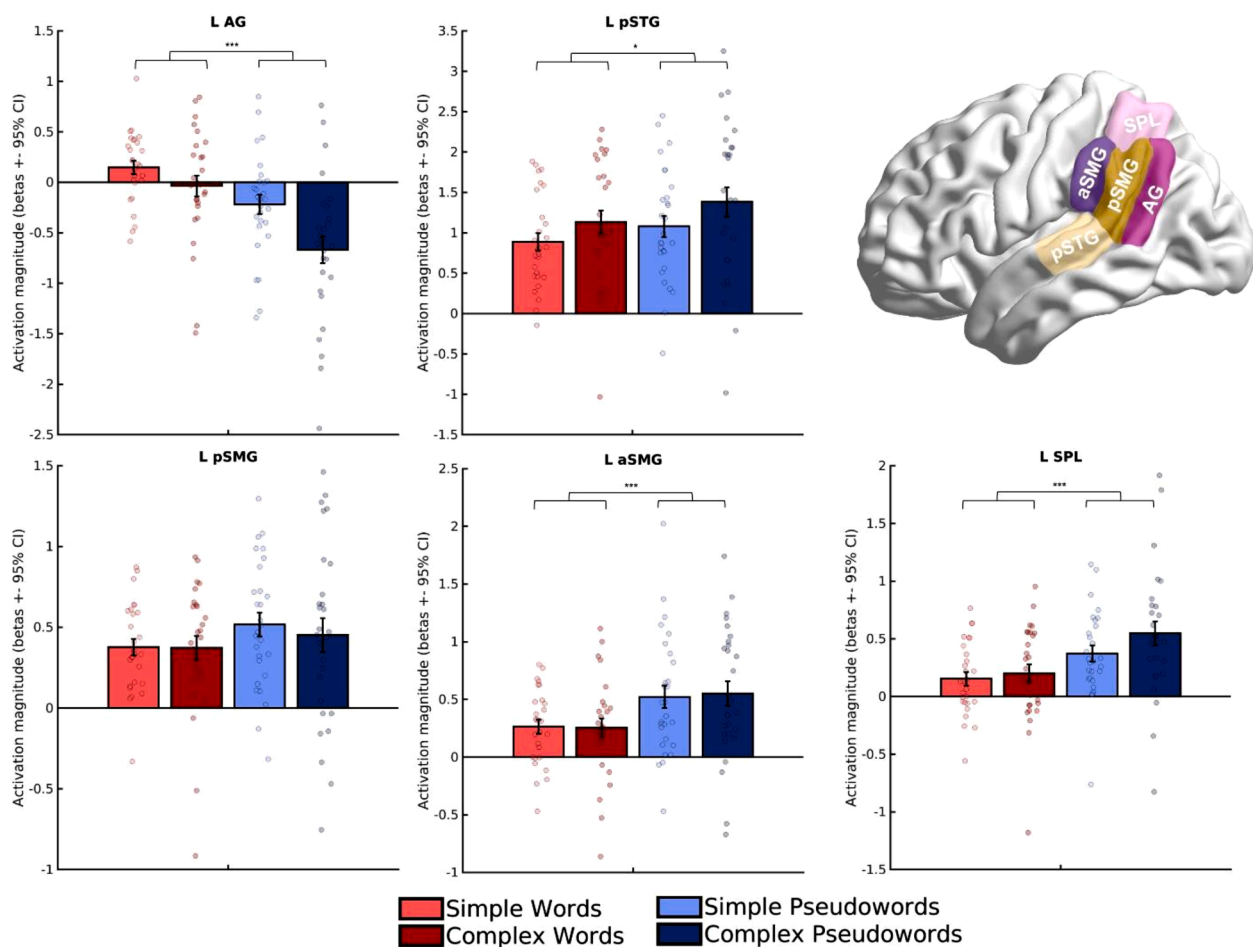


**Fig. 3.** *Activation magnitude for the four conditions in subregions of the left TPC.* Based on clusters derived from the Harvard-Oxford atlas, we compared activation magnitude in each participant in five designated ROIs (left AG, left pSTG, left pSMG, left aSMG and left SPL) during the four respective conditions: simple word, complex word, simple pseudoword and complex pseudoword reading. Repeated measures ANOVAs for each ROI were computed and significant main effects of stimulus type (i.e., significant differences in recruitment during word and pseudoword reading) are explicitly marked in the respective plots (*** $p < .001$, ** $p < .01$, * $p < .05$). Only left AG showed higher word-specific recruitment, whereas left aSMG, left pSTG and left SPL showed stronger recruitment during pseudoword reading. Apart from marked word type effects, main effects of complexity were also significant in left AG, left pSTG and left SPL. In contrast to left AG, the other two regions showed higher activation for complex stimuli.
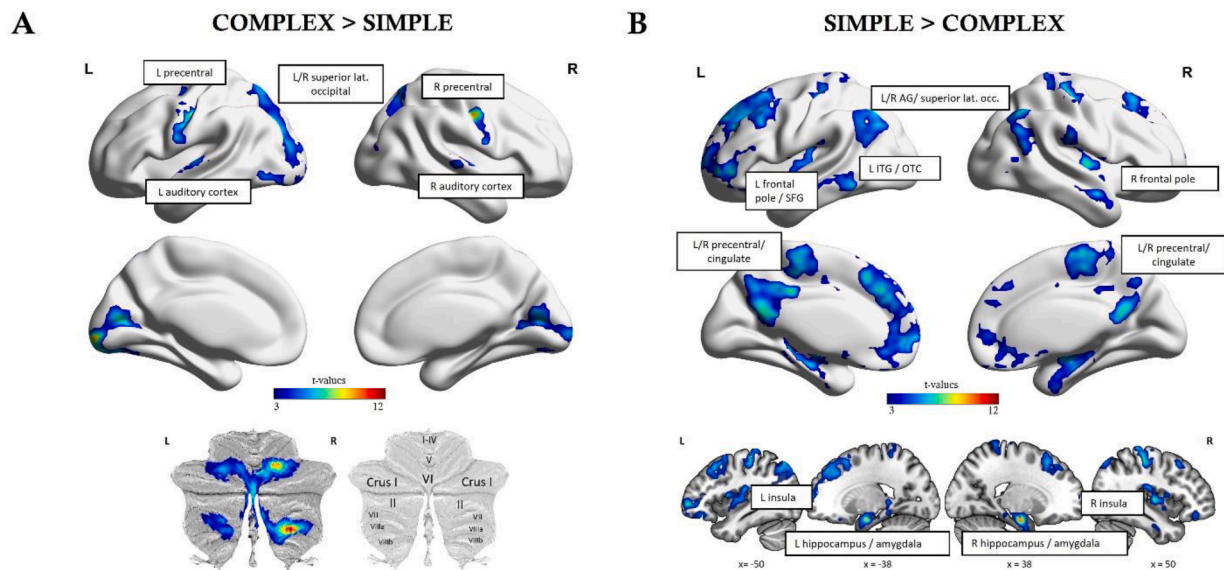
**Fig. 4.** *Cortical and cerebellar findings for the processing of simple and complex stimuli.* (A) Complex > simple stimuli (averaged across stimulus types), (B) simple > complex stimuli (averaged across stimulus types). We display results for the cerebral cortex and the cerebellum during the sham (i.e., placebo) condition, corrected at $p < .001$ voxel-level and FWE-cluster-corrected at $p < .05$. Please note that no significant cluster in the cerebellum was found for (B), which is why no cerebellar flatmap for this contrast is shown.

effects for complexity ($z = 5.800$, $p < .001$) and stimulus type ($z = 2.027$, $p = .043$). The pseudoword-complexity interaction was also significant ($z = 11.02$, $p < .001$), revealing again significant differences for simple vs. complex words ($t = -5.922$, $p < .0001$), simple vs. complex pseudowords ($t = -16.197$, $p < .0001$), simple words vs. simple pseudowords ($t = -2.515$, $p = .0119$) and complex words vs. complex pseudowords ($t = -18.115$, $p < .0001$) (see Tables S4 and S5). Likewise, we found a main effect for stimulus type ($z = -3.196$, $p = .001$) and a significant complexity-by-pseudoword interaction ($z = -3.392$, $p < .001$) for reading accuracy. Post-hoc tests revealed significant differences in accuracy for simple vs. complex pseudowords ($t = 3.998$, $p = .0001$) and for complex words vs. complex pseudowords ($t = 6.919$, $p < 0.0001$).
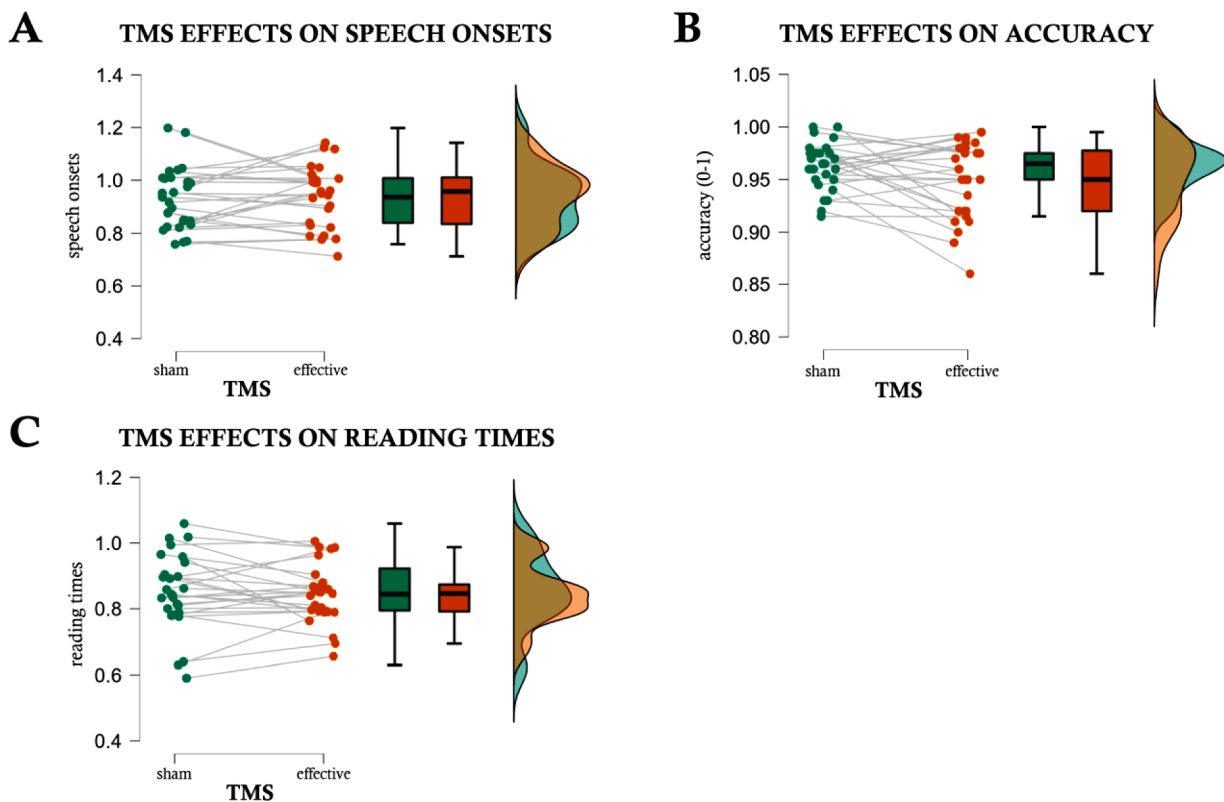


**Fig. 5.** *Individual differences in TMS response on the behavioural level.* Figures A, B and C show non-significant findings of TMS on speech onsets, accuracy and reading times (across all stimuli). We suggest that a lack of group-level findings stems from large individual variability across subjects and differential effects of TMS on reading performance.

Differences between simple and complex words and simple words and pseudowords were not significant (see details in Tables S6 and S7).

Regarding TMS effects, we found no main effect of TMS on speech onsets ($z = 0.718$, $p = .473$, n.s.), reading times ($z = 1.133$, $p = .257$, n. s.) or accuracy ($z = 0.001$, $p = .999$, n.s.). There was only a weak interaction for TMS, complexity, stimulus type and session for speech onsets ($z = 2.07$, $p = .04$), with post-hoc tests showing that when effective TMS was performed in the second session, subjects had increased speech onsets for complex words ($t = 2.083$, $p = .037$) (Table S2). We did not find any TMS effects on reading times and accuracy (all $p > .05$; see Fig. 5), most likely due to large variability in TMS responses, with some individuals getting better, some worse on an individual level.

### 3.3. TMS effects on functional activation

Regarding TMS effects on brain function, univariate whole-brain analyses showed no significant differences in brain activation between effective and sham TMS on the group-level. To better understand this lack of group-level findings, we performed an exploratory subject-specific analysis with individual subject maps thresholded at $p < .001$ (uncorrected) (Fig. 6). Supporting our observation of large inter-individual variability in behavioural response to TMS, participants also showed large differences in univariate brain activation involving up- or down-regulation of the bilateral motor cortices and occipital lobes following effective TMS. In other words, the same regions showed up- or down-regulation following TMS in different subjects.

Since univariate analyses are insensitive to fine-grained differences in multi-voxel activity patterns (Mur et al., 2009), we additionally performed MVPA decoding to investigate the effect of TMS on functional activation patterns. To this end, we moved a 5-mm "searchlight" through the entire brain, training a machine-learning classifier to distinguish effective vs. sham TMS based on the local activity patterns of n-1 subjects, and testing the classifier on the remaining subject (i.e., leave-one-subject-out cross-validation). We found significant above-chance decoding (>50%) selectively for pseudowords and selectively in a cluster covering portions of the left IFG (pars triangularis), extending to the inferior frontal sulcus (peak: x, y, z = -42 30 20) (Fig. 7) (see a discussion on the role of the IFG regions for pseudowords in Turker and Hartwigsen (2021)). No effects were observed for word reading.

### 3.4. TMS-induced effects on effective connectivity

We used DCM to explore TMS-induced changes in effective connectivity within the reading network, including the three core reading areas: left IFG, left TPC and left vOTC (Fig. 8). We found strong inter-regional connectivity, and pseudowords drove all three regions more strongly than words (Bayesian contrasts for TPC: $Pp = 0.999$; IFG: $Pp = 1.0$; vOTC: $Pp = 1.0$). Crucially, effective connectivity from the left vOTC to the left TPC was significantly increased by effective TMS over the left TPC across both reading conditions (modulation: 0.699; result: 0.464 Hz). This modulation was stronger for effective than for sham TMS (modulation: 0.349; result: 0.113 Hz; Bayesian contrast between effective and sham TMS: $Pp = 1.0$).

## 4. Discussion

Here, we tested how perturbation of the left TPC with TMS prior to functional neuroimaging affects network activity, task-related
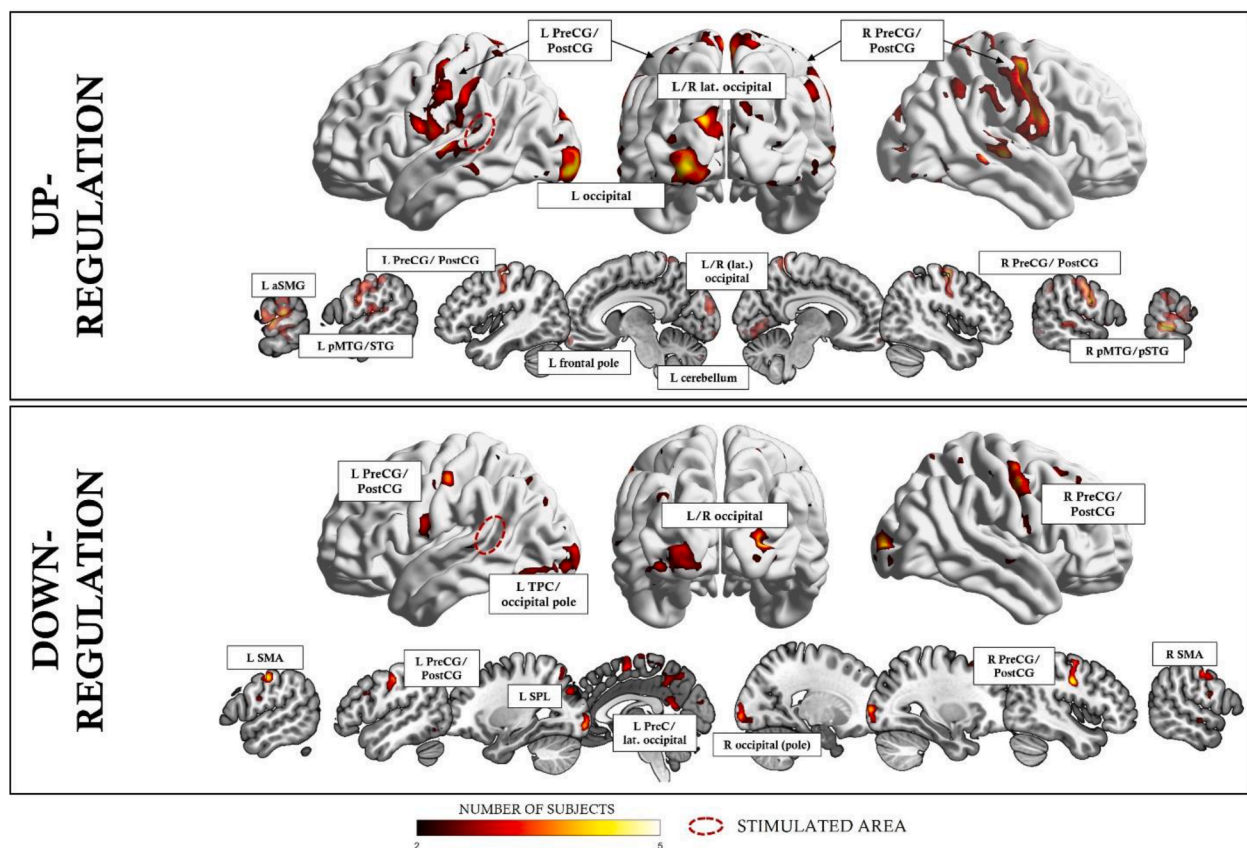


**Fig. 6.** Subject-specific up- or down-regulation of functional activation for effective vs. sham TMS. Overlap of subject-specific activation maps for effective vs. sham stimulation (p<.001 uncorrected at the voxel level, thresholded at 2 subjects; color indicates number of subjects showing activation increase/decrease in the same voxel). The upper panel shows up-regulation, i.e., higher activation after effective when compared to sham stimulation. The lower panel shows down-regulation, i.e., lower activity after effective than sham TMS.
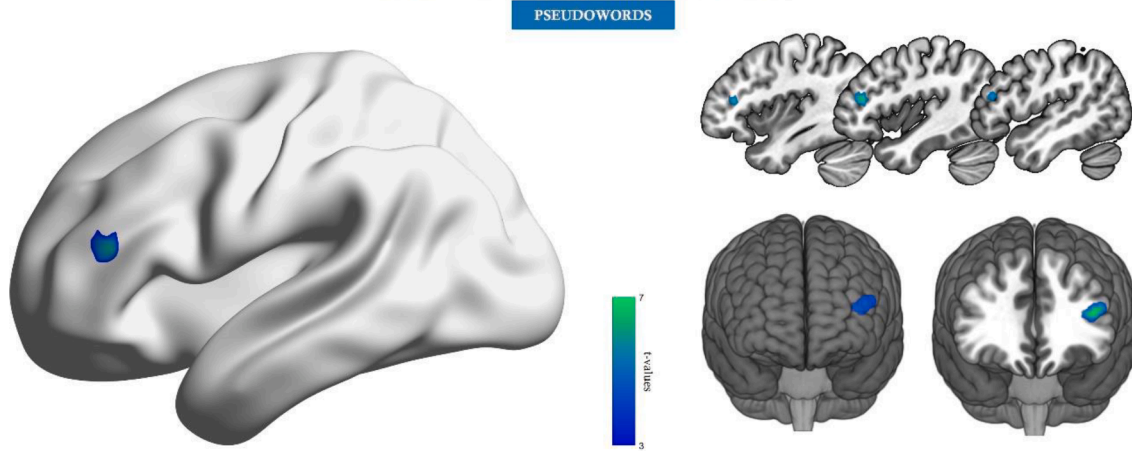
**Fig. 7.** *Results for between-subject searchlight MVPA showing TMS-induced differences in activation during pseudoword reading.* Following effective stimulation of the left TPC as compared to sham stimulation, we found a shift in functional activation patterns in the left IFG (pars triangularis) / inferior frontal sulcus selectively for pseudoword reading. The marked area showed above-chance decoding accuracy (>50%) for effective vs. sham stimulation. We report non-parametric t-values as provided by the SnPM toolbox (Nichols, 2023).
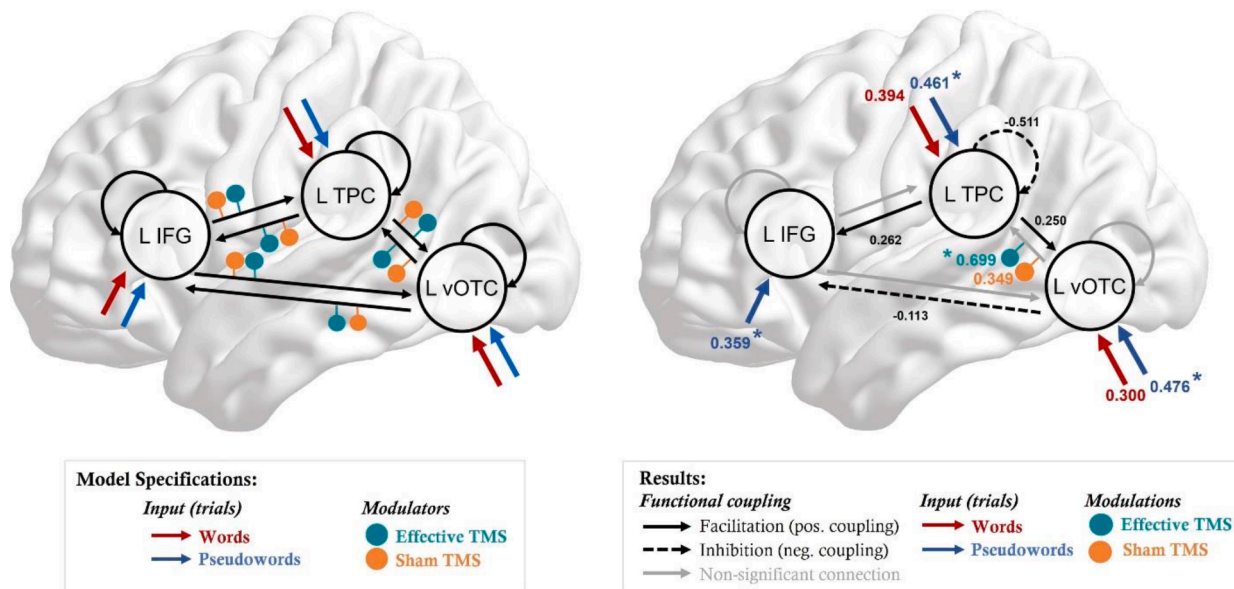


**Fig. 8.** *Dynamic causal modeling results.* Left side: The "full" DCM model that served as starting point for Bayesian model reduction. Black arrows represent intrinsic connections, colored arrows denote driving inputs, and coloured dots represent modulators. Right side: The resulting Bayesian Model Average thresholded at 99% parameter probability. Driving inputs and between-region functional coupling are in Hz. Modulators in- or decrease connections in an additive manner. *: Significantly stronger modulation than other parameters ($Pp > 0.99$).

connectivity, and performance during word and pseudoword reading in typical adult readers. Our main findings were as follows. First, left TPC subregions and the cerebellum are differentially recruited for word and pseudoword reading and the processing of complex stimuli. Second, TMS-induced effects on reading performance and brain activation showed strong variability across subjects without any clear pattern at the behavioural or neural level when using standard univariate analyses. However, multivariate analyses revealed a shift in activation in the left inferior frontal cortex for pseudoword reading following TMS-induced disruption. Furthermore, we found increased effective connectivity from the left vOTC to the targeted left TPC after TMS. The observed changes in task-related activity and the increase in functional coupling between two core reading nodes suggest successful short-term

compensatory reorganization in the reading network following TMS-induced disruption. These changes may have prevented behavioural disruption.

### 4.1. Left TPC regions are differentially engaged during word and pseudoword reading

We first explored differences in task-related activity during word and pseudoword reading at baseline (i.e., after sham TMS). Whereas left AG was more engaged during word reading, three other subregions within the left TPC showed a strong preference for pseudowords. Earlier reading studies found largely overlapping activation patterns for words and pseudowords (e.g., Danelli et al., 2013), which stands in contrast to

our findings. Since sight word reading is an automatized, higher-order cognitive task that relies upon lexical retrieval and semantic access (Numssen et al., 2021), it is expected that word reading recruits the left AG (see summaries by Davis, 2016; Seghier, 2023). We provide evidence for this by directly linking left AG activation to word reading, with deactivation of that region during pseudoword reading (Kuhnke et al., 2022; Kuhnke, Kiefer, et al., 2020). Based on our results, we suggest a functional specialization of the left TPC, with left aSMG, left pSTG and left SPL showing significantly stronger engagement during pseudoword when compared to word reading. Our findings corroborate earlier findings by Oberhuber et al. (2016), who found the most superior portion of SMG (aSMG extending to the left SPL in our ROIs) to be active during visual pseudoword tasks, which they attributed to a cognitive cluster of executive processing. Moreover, they linked word processing to a dorsal portion of the SMG, which corresponds more closely to the pSMG / AG region in the Harvard-Oxford atlas as chosen in our study. While the left SPL might not be a classical reading region, its role for letter processing and attentional demands was recently confirmed in NIBS studies (Turker & Hartwigsen, 2021). We suggest that its contribution to pseudoword reading in our current study might stem from increased attentional demand and phoneme-grapheme conversion during the pseudoword reading process.

### 4.2. Longer and more complex items show increased activation in left pSTG and left SPL

We also looked at the effects of complexity (i.e., by comparing simple and complex items). Whereas left AG showed a negative effect for complexity, with stronger deactivation for more complex stimuli across both words and pseudowords, left pSTG and left SPL showed stronger engagement during the reading of complex items. This is particularly interesting since it might reflect higher articulatory demands and more demanding access to the phonological lexicon in the case of left STG (Peramunage et al., 2011). In the case of left SPL, in contrast, the increased activation for complex stimuli could be interpreted as higher attentional and visual demand (Valdois et al., 2019), which is in line with its pseudoword-specific recruitment.

### 4.3. The role of the cerebellum for word, pseudoword and complexity processing in typical readers

In the direct contrast between conditions (pseudowords vs. words), we found that words showed significantly stronger engagement of crus I and II in both hemispheres, whereas pseudowords also recruited bilateral crus II, lobules VI, VIIIa and VIIIb. These findings are partially in line with a recent large-scale meta-analysis linking these regions within the cerebellum to language and more specifically to semantic and phonological processing (Turker et al., 2023). Additionally, that meta-analysis found that specifically lobule VI was more engaged in overt tasks. A meta-analysis focussing on the role of the cerebellum suggested that motor activation might be reflected in lobule VIIIa / VIIIb activation, whereas other studies linked lobules VIIb and VIIIa to load-dependent activity in visual working memory (Brissenden et al., 2021). Our current study provides evidence for a link to visual working memory since complex stimuli, that are more demanding in terms of visual processes and working memory, showed the highest activation peak across all clusters in the right cerebellum lobule VIIIa. Smaller clusters for complex stimuli were situated in the left cerebellum VIIb and VIIIa. Stoodley & Schmahmann (2009) had found that cerebellar activation for cognitive processes (e.g., language, working memory) involved the posterior but not the anterior lobes of the cerebellum, which we cannot corroborate in our current study, where anterior lobes (crus I and II) also showed task-specific engagement. Similarly, Kuhnke, Kiefer, et al. (2020) found task-specific multimodal effects in right crus I / II during conceptual-semantic tasks on written words.

### 4.4. Inhibition of left TPC does not significantly affect reading performance

One of the main aims of the present study was to explore whether the left TPC, a critical region for acquiring and establishing sound-letter mappings, is causally involved in reading processing in adult readers. Electrical field simulations (see Fig. 1) showed that we successfully stimulated the targeted area across participants, with strongest stimulation effects at the intersection of left aSMG, left pSMG and left pSTG. Two of these areas showed pseudoword-specific recruitment during the task, emphasizing their relevance for pseudoword reading. Only two studies have investigated the effects of TMS of the left TPC on reading. The first study reported higher pseudoword accuracy after left inferior parietal lobe stimulation, and lower text reading accuracy after left pSTG stimulation (Costanzo et al., 2012a). We believe that the differences to our study could stem from a more precise neuronavigation in the present study, which may have resulted in targeting a different (sub-)region, more complex / longer stimuli, a larger sample size and differences in stimulation parameters (cTBS instead of high frequency rTMS). Moreover, while facilitatory TMS effects on task performance are often interpreted as causal evidence for the contribution targeted areas, such effects could also reflect the inhibition of task-irrelevant areas that compete for resources (Bergmann & Hartwigsen, 2021; Luber & Lisanby, 2014). In a language mapping study by Hauck and colleagues (Hauck et al., 2015a, 2015b), several regions were targeted but no strong effect of TMS on the TPC for pseudoword reading could be observed. We reason that the absence of a strong behavioural TMS effect in our study may be explained by the observed short-term plasticity at the network level after stimulation, which may have compensated for the disruption and helped to maintain task performance at a relatively high level (see 4.5 below for discussion). Moreover, we found large individual variability, with some individuals showing a disruption, others showing improvements after TMS-induced disruption of left TPC.

### 4.5. Large individual variability in the neural response to TMS

Our investigation of individual differences in functional activation differences induced by TMS suggests large individual variability even within the same brain regions. It is striking that up- and down-regulation of task-related activity affected largely overlapping areas. In other words, some individuals responded with more and others with less activation in the bilateral motor areas, portions of the STG, and occipital areas in response to effective TMS. These analyses showed that neural responses to TMS differed considerably between individuals, which might explain the lack of group-level differences on the neural and behavioural level. Whereas the investigation of inter-individual variability in behavioural response to TMS has gained momentum in the past years (Corp et al., 2021; López-Alonso et al., 2014), variability in neurophysiological response has not been studied to our knowledge.

### 4.6. Multivariate analyses reveal a TMS-induced modulation of the left IFG

Our univariate analyses did not reveal any group-level differences in functional activation on the voxel level. In contrast, MVPA indicated that effective TMS over the left TPC altered fine-grained multi-voxel activity patterns for pseudoword reading in an inferior frontal cluster. The involvement of an anterior portion of left IFG including the inferior frontal sulcus is surprising given that previous studies relate left BA 44 to grapheme-phoneme conversion, and left BA 45 rather to explicit lexical search (Heim et al., 2005). However, theories hold that the larger IFG region is also crucial for phonological output resolution and rhyming during (MacSweeney et al., 2009; Taylor et al., 2013) as well as attention and working memory (Corbetta & Shulman, 2002; Tops & Boksem, 2011). With pseudowords having a higher decoding demand and thus requiring more processing effort, it is likely that differences in response

patterns of the left IFG at least partially stem from higher demands on attention, executive functions, and cognitive control. Considering the overlap of our cluster with the inferior frontal sulcus, this explanation seems plausible. Alternatively, the stronger contribution of left IFG to pseudoword reading after disruption of the left TPC might also reflect a shift in balance towards another key node for reading, and thus reflect phonological processes per se. This explanation would be in line with previous TMS studies showing flexible redistribution between homologous areas (e.g., Hartwigsen et al., 2013; Jung & Lambon Ralph, 2016) or remote regions from the same specialized subnetwork (Hallam et al., 2016) during different language tasks (Hartwigsen, 2016). Thus, a stronger contribution of the left IFG likely reflects compensatory attempts in the network which helped to maintain task processing at a high level and may have prevented decreases in task accuracy. While the absence of a TMS-induced modulation of task-related activation in the stimulated area may be surprising, previous work demonstrated compensatory reorganization in distributed networks after inhibitory TMS for language and other cognitive tasks (Hartwigsen, Bzdok, et al., 2017; Hartwigsen & Volz, 2021). Such remote stimulation effects (e.g., Herz et al., 2014) in connected areas in the absence of a modulatory effect at the stimulation site are thus not completely surprising (Farcy et al., 2022). We note that the two alternative explanations (increased task demands during pseudoword reading vs. redistribution within the phonological network) are not mutually exclusive, and both mechanisms may have contributed to the observed changes in left IFG activity.

### 4.7. TMS increases task-specific functional coupling in the reading network

The results of our DCM analysis including the three core reading nodes as defined by the literature suggest that a disruption of the left TPC resulted in a stronger facilitatory drive from the left vOTC to the left TPC. This, in turn, suggests a TMS-induced up-regulation in the form of a compensatory mechanism. This is particularly interesting since the left vOTC plays a key role in orthographic processing and is vital for reading words and pseudowords (Jobard et al., 2003; Turker & Hartwigsen, 2021). A functional engagement of this region for pseudoword processing could also be confirmed in the univariate analyses of this study. The observed increase in the facilitatory influence of the left vOTC on the left TPC during pseudoword processing after TMS could be interpreted as short-term adaptation or compensation. As such, functional connectivity between these two areas is most likely vital for successful and efficient decoding, so that a disruption of the left TPC requires an up-regulation of functional coupling to compensate for the increased demand posed by the task. This highlights the importance of considering within-network interactions when exploring TMS-induced effects on the neural level, especially in the absence of a modulatory effect in the stimulated area. When considering TMS-induced changes on task-related activity and connectivity, it is important to bear in mind that TMS is not "lesioning" an area and unlikely to completely "silence" processing in the targeted region. Consequently, a shift in the balance between different nodes in the respective network with a stronger contribution of another area may help to maintain processing at a relatively high level despite disruption (see Hartwigsen, 2018).

### 4.8. TMS-induced changes in functional activation and connectivity suggest compensation within the reading network to sustain reading

The present study is the first study that mapped TMS-induced behavioural changes on reading performance on the neural level with fMRI. Earlier research on language skills suggests that TMS leads to plastic after-effects, such as large-scale changes on the network level affecting both local and remote activity within targeted networks, as well as interactions between other involved networks (Hartwigsen & Volz, 2021). As such, the perturbed brain can flexibly redistribute and functionally reorganize its computational capacities to compensate for

the disruption of an area or network. The present study adds first evidence for compensatory mechanisms within the typical reading network in terms of functional brain activation.

Based on our results we suggest that the TPC is crucial for pseudoword processing. However, the reading network in typical adult readers is flexible enough to adapt to the disruption by increasing functional coupling between the left vOTC and the left TPC, and at the same time shifting functional activation in the left IFG. Based on our lack of behavioural findings, we assume that the reading network is well equipped to accommodate the induced disruption. Nevertheless, we initially expected inhibitory TMS effects at the stimulation site and in the reading network. The absence of any direct stimulation effects in the TPC was surprising. However, it is not uncommon that studies find no effects under the coil or stronger stimulation in remote areas (Bergmann et al., 2016; Bergmann & Hartwigsen, 2021). Of note, it is currently unclear whether such remote effects are caused by local synaptic plasticity in the target site, subsequently affecting remote activity via changes in functional connectivity or via synaptic plasticity in the remote site itself induced by spread of activity during the stimulation. Even in the presence of local effects at the stimulation site, some combined TMS-fMRI studies reported that the behavioural relevance of these effects was linked to remote effects (Hartwigsen, Bzdok, et al., 2017; Herz et al., 2014). Since the strongest remote effects in our study were found in the left IFG, we may speculate that targeting this area may be more promising to modulate underlying network activity and potentially also behavior.

### 4.9. Insight into the reading network(s) through neurostimulation

With respect to the contribution of our data to theoretical reading models, our study can be explained under the framework of two reading models, one being the connectionist framework of reading (Seidenberg, 2005), the other the dual-cascaded model of reading (DRC; Coltheart, 2006; Coltheart et al., 2001). Due to the lack of high temporal resolution with fMRI, our findings cannot provide evidence for a hierarchical organization of the reading network. However, we believe that they support a constant interaction between reading areas, in line with connectionist accounts. Furthermore, our findings highlight that decoding recruits the left TPC, which is in line with earlier assumptions that unfamiliar word and pseudoword reading rely upon a dorsal reading stream, including recruitment of the vOTC, the left TPC and the left IFG (backed by structural connectivity research, e.g., Cummine et al., 2015). Since we did not observe any effects on word processing, words might recruit a different route that does not require the left TPC or might be too automatized and robustly presented in the semantic lexicon as to respond to a TMS-induced disruption in the left TPC.

## 5. Conclusion

By combining rTMS with fMRI, we found that a disruption of the left TPC in healthy readers led to (1) a change in functional activity patterns in the left IFG, and (2) an increase of functional coupling between the left vOTC and the left TPC. Due to the lack of a behavioural effect of TMS, we interpret these two neurophysiological effects as compensatory mechanisms to sustain reading. Even though we only used a single session intervention in this study, we could still see immediate effects on the neural levels. This study is thus the first to report adaptive plasticity within the reading network in response to perturbation. The present findings can guide future studies and suggest new perspectives concerning the treatment of reading disorders, e.g., by designing multiple-session interventions for individuals with reading impairments. Overall, our study advances future experimental and translational applications of TMS in health and disease.

## Data availability

I have already shared the osf link that will be used for all available data and code.

*Data and code availability statements*

All data and code is available at the following OSF registry: osf.io/ fpgcy (Turker & Kuhnke, 2023).

## Supplementary materials

Supplementary material associated with this article can be found, in the online version, at doi:10.1016/j.neuroimage.2023.120373.

## References

Audacity Team. (2021). *Audacity (R): free audio editor and recorder* [Computer software]. www.audacityteam.org.

Barr, D.J., Levy, R., Scheepers, C., Tily, H.J., 2013. Random effects structure for confirmatory hypothesis testing: keep it maximal. J. Mem. Lang. 68 (3) https://doi.org/10.1016/j.jml.2012.11.001, 10.1016/j.jml.2012.11.001.

Behzadi, Y., Restom, K., Liau, J., Liu, T.T., 2007. A component based noise correction method (CompCor) for BOLD and perfusion based fMRI. Neuroimage 37 (1), 90–101. https://doi.org/10.1016/j.neuroimage.2007.04.042.

Bergmann, T.O., Hartwigsen, G., 2021. Inferring causality from noninvasive brain stimulation in cognitive neuroscience. J. Cogn. Neurosci. 33 (2), 195–225. https://doi.org/10.1162/jocn_a_01591.

Bergmann, T.O., Karabanov, A., Hartwigsen, G., Thielscher, A., Siebner, H.R., 2016. Combining non-invasive transcranial brain stimulation with neuroimaging and electrophysiology: Current approaches and future perspectives. Neuroimage 140, 4–19. https://doi.org/10.1016/j.neuroimage.2016.02.012.

Boersma, P., & Weening, D. (2021). *Praat: doing phonetics by computer* (6.1.38) [Computer software].

Brissenden, J.A., Tobyne, S.M., Halko, M.A., Somers, D.C., 2021. Stimulus-specific visual working memory representations in human cerebellar lobule VIIb/VIIIa. J. Neurosci. 41 (5), 1033–1045. https://doi.org/10.1523/JNEUROSCI.1253-20.2020.

Brooks, M., E., Kristensen, K., Benthem, K., J., van, Magnusson, A., Berg, C., W., Nielsen, A., Skaug, H., J., Mächler, M., Bolker, B., M., 2017. GlmmTMB balances speed and flexibility among packages for zero-inflated generalized linear mixed modeling. R J. 9 (2), 378. https://doi.org/10.32614/RJ-2017-066.

Chyl, K., Fraga-González, G., Brem, S., Jednoróg, K., 2021. Brain dynamics of (a)typical reading development—a review of longitudinal studies. Npj Sci. Learn. 6 (1) https://doi.org/10.1038/s41539-020-00081-5. Article 1.

Coltheart, M., 2006. Dual route and connectionist models of reading: an overview. London Rev. Educ. https://doi.org/10.1080/13603110600574322.

Coltheart, M., Rastle, K., Perry, C., Langdon, R., Ziegler, J., 2001. DRC: a dual route cascaded model of visual word recognition and reading aloud. Psychol. Rev. 108 (1), 204–256. https://doi.org/10.1037/0033-295X.108.1.204.

Corbetta, M., Shulman, G.L., 2002. Control of goal-directed and stimulus-driven attention in the brain. Nat. Rev. Neurosci. 3 (3) https://doi.org/10.1038/nrn755. Article 3.

Corp, D.T., Bereznicki, H.G.K., Clark, G.M., Youssef, G.J., Fried, P.J., Jannati, A., Davies, C.B., Gomes-Osman, J., Kirkovski, M., Albein-Urios, N., Fitzgerald, P.B., Koch, G., Di Lazzaro, V., Pascual-Leone, A., Enticott, P.G., 2021. Large-scale analysis of interindividual variability in single and paired-pulse TMS data. Clin. Neurophysiol. 132 (10), 2639–2653. https://doi.org/10.1016/j.clinph.2021.06.014.

R Core Team, 2022. *R: A language and Environment for Statistical Computing.* [Computer Software]. R Foundation for Statistical Computing. https://www.R-project.org/.

Costanzo, F., Menghini, D., Caltagirone, C., Oliveri, M., Vicari, S., 2012a. High frequency rTMS over the left parietal lobule increases non-word reading accuracy. Neuropsychologia 50 (11), 2645–2651. https://doi.org/10.1016/j.neuropsychologia.2012.07.017.

Costanzo, F., Menghini, D., Caltagirone, C., Oliveri, M., Vicari, S., 2012b. High frequency rTMS over the left parietal lobule increases non-word reading accuracy. Neuropsychologia 50 (11), 2645–2651. https://doi.org/10.1016/j.neuropsychologia.2012.07.017.

Costanzo, F., Menghini, D., Caltagirone, C., Oliveri, M., Vicari, S., 2013. How to improve reading skills in dyslexics: The effect of high frequency rTMS. Neuropsychologia 51 (14), 2953–2959. https://doi.org/10.1016/j.neuropsychologia.2013.10.018.

Costanzo, F., Rossi, S., Varuzza, C., Varvara, P., Vicari, S., Menghini, D., 2019. Long-lasting improvement following tDCS treatment combined with a training for reading in children and adolescents with dyslexia. Neuropsychologia 130, 38–43. https://doi.org/10.1016/j.neuropsychologia.2018.03.016.

Cummine, J., Dai, W., Borowsky, R., Gould, L., Rollans, C., Boliek, C., 2015. Investigating the ventral-lexical, dorsal-sublexical model of basic reading processes using diffusion tensor imaging. Brain Struct. Funct. 220 (1), 445–455. https://doi.org/10.1007/s00429-013-0666-8.

Danelli, L., Berlingeri, M., Bottini, G., Ferri, F., Vacchi, L., Sberna, M., Paulesu, E., 2013. Neural intersections of the phonological, visual magnocellular and motor/cerebellar systems in normal readers: Implications for imaging studies on dyslexia. Hum. Brain Mapp. 34 (10), 2669–2687. https://doi.org/10.1002/hbm.22098.

Davis, M.H, 2016. Chapter 44—the neurobiology of lexical access. In: Hickok, G., Small, S.L. (Eds.), Neurobiology of Language. Academic Press, pp. 541–555. https://doi.org/10.1016/B978-0-12-407794-2.00044-4.

Dehaene, S., Cohen, L., 2011. The unique role of the visual word form area in reading. Trends Cogn. Sci. 15 (6), 254–262. https://doi.org/10.1016/j.tics.2011.04.003.

Desikan, R.S., Ségonne, F., Fischl, B., Quinn, B.T., Dickerson, B.C., Blacker, D., Buckner, R.L., Dale, A.M., Maguire, R.P., Hyman, B.T., Albert, M.S., Killiany, R.J., 2006. An automated labeling system for subdividing the human cerebral cortex on MRI scans into gyral based regions of interest. Neuroimage 31 (3), 968–980. https://doi.org/10.1016/j.neuroimage.2006.01.021.

Devlin, J.T., Matthews, P.M., Rushworth, M.F.S., 2003. Semantic processing in the left inferior prefrontal cortex: a combined functional magnetic resonance imaging and transcranial magnetic stimulation study. J. Cogn. Neurosci. 15 (1), 71–84. https://doi.org/10.1162/089892903321107837.

Duncan, K.J., Pattamadilok, C., Devlin, J.T., 2010. Investigating occipito-temporal contributions to reading with TMS. J. Cogn. Neurosci. 22 (4), 739–750. https://doi.org/10.1162/jocn.2009.21207.

Ehri, L.C., 2005. Learning to read words: theory, findings, and issues. Sci. Stud. Read. 9 (2), 167–188. https://doi.org/10.1207/s1532799xssr0902_4.

Farcy, C., Moliadze, V., Nees, F., Hartwigsen, G., Guggisberg, A.G., 2022. Identifying neural targets for enhancing phonological processing with transcranial alternate current stimulation. Brain Stimul.: Basic, Transl. Clin. Res. Neuromodul. 15 (3), 789–791. https://doi.org/10.1016/j.brs.2022.05.009.

Faul, F., Erdfelder, E., Lang, A.-G., Buchner, A., 2007. G*Power 3: A flexible statistical power analysis program for the social, behavioral, and biomedical sciences. Behav. Res. Methods 39 (2), 175–191. https://doi.org/10.3758/BF03193146.

Frazier, J.A., Chiu, S., Breeze, J.L., Makris, N., Lange, N., Kennedy, D.N., Herbert, M.R., Bent, E.K., Koneru, V.K., Dieterich, M.E., Hodge, S.M., Rauch, S.L., Grant, P.E., Cohen, B.M., Seidman, L.J., Caviness, V.S., Biederman, J., 2005. Structural brain magnetic resonance imaging of limbic and thalamic volumes in pediatric bipolar disorder. Am. J. Psychiatry 162 (7), 1256–1265. https://doi.org/10.1176/appi.ajp.162.7.1256.

Friston, K.J., Harrison, L., Penny, W., 2003. Dynamic causal modelling. Neuroimage 19 (4), 1273–1302. https://doi.org/10.1016/S1053-8119(03)00202-7.

Friston, K.J., Litvak, V., Oswal, A., Razi, A., Stephan, K.E., van Wijk, B.C.M., Ziegler, G., Zeidman, P., 2016. Bayesian model reduction and empirical Bayes for group (DCM) studies. Neuroimage 128, 413–431. https://doi.org/10.1016/j.neuroimage.2015.11.015.

Friston, K.J., Williams, S., Howard, R., Frackowiak, R.S.J., Turner, R., 1996. Movement-Related effects in fMRI time-series. Magn. Reson. Med. 35 (3), 346–355. https://doi.org/10.1002/mrm.1910350312.

Gagl, B., Sassenhagen, J., Haan, S., Gregorova, K., Richlan, F., Fiebach, C.J., 2020. An orthographic prediction error as the basis for efficient visual word recognition. Neuroimage 214, 116727. https://doi.org/10.1016/j.neuroimage.2020.116727.

Goldstein, J.M., Seidman, L.J., Makris, N., Ahern, T., O'Brien, L.M., Caviness, V.S., Kennedy, D.N., Faraone, S.V., Tsuang, M.T., 2007. Hypothalamic abnormalities in schizophrenia: Sex effects and genetic vulnerability. Biol. Psychiatry 61 (8), 935–945. https://doi.org/10.1016/j.biopsych.2006.06.027.

Gough, P.M., Nobre, A.C., Devlin, J.T., 2005. Dissociating linguistic processes in the left inferior frontal cortex with transcranial magnetic stimulation. J. Neurosci. 25 (35), 8010–8016. https://doi.org/10.1523/JNEUROSCI.2307-05.2005.

Hallam, G.P., Whitney, C., Hymers, M., Gouws, A.D., Jefferies, E., 2016. Charting the effects of TMS with fMRI: Modulation of cortical recruitment within the distributed network supporting semantic control. Neuropsychologia 93 (February), 40–52. https://doi.org/10.1016/j.neuropsychologia.2016.09.012.

Hartwigsen, G., 2016. Adaptive plasticity in the healthy language network: implications for language recovery after stroke. Neural Plast. 2016 https://doi.org/10.1155/2016/9674790.

Hartwigsen, G., 2018. Flexible redistribution in cognitive networks. Trends Cogn. Sci. 22 (8), 687–698. https://doi.org/10.1016/j.tics.2018.05.008.

Hartwigsen, G., Baumgaertner, A., Price, C.J., Koehnke, M., Ulmer, S., Siebner, H.R., 2010a. Phonological decisions require both the left and right supramarginal gyri. Proc. Natl. Acad. Sci. USA. 107 (38), 16494–16499. https://doi.org/10.1073/pnas.1008121107.

Hartwigsen, G., Bzdok, D., Klein, M., Wawrzyniak, M., Stockert, A., Wrede, K., Classen, J., Saur, D., 2017a. Rapid short-term reorganization in the language network. eLife 6, e25964. https://doi.org/10.7554/eLife.25964.

Hartwigsen, G., Henseler, I., Stockert, A., Wawrzyniak, M., Wendt, C., Klingbeil, J., Baumgaertner, A., Saur, D., 2017b. Integration demands modulate effective connectivity in a fronto-temporal network for contextual sentence integration. Neuroimage 147, 812–824. https://doi.org/10.1016/j.neuroimage.2016.08.026.

Hartwigsen, G., Price, C.J., Baumgaertner, A., Geiss, G., Koehnke, M., Ulmer, S., Siebner, H.R., 2010b. The right posterior inferior frontal gyrus contributes to phonological word decisions in the healthy brain: Evidence from dual-site TMS. Neuropsychologia 48 (10), 3155–3163. https://doi.org/10.1016/j.neuropsychologia.2010.06.032.

Hartwigsen, G., Saur, D., Price, C.J., Ulmer, S., Baumgaertner, A., Siebner, H.R., 2013. Perturbation of the left inferior frontal gyrus triggers adaptive plasticity in the right homologous area during speech production. Proc. Natl. Acad. Sci. USA. 110 (41), 16402–16407. https://doi.org/10.1073/pnas.1310190110.

Hartwigsen, G., Volz, L.J., 2021. Probing rapid network reorganization of motor and language functions via neuromodulation and neuroimaging. Neuroimage 224 (April 2020), 117449. https://doi.org/10.1016/j.neuroimage.2020.117449.

Hauck, T., Tanigawa, N., Probst, M., Wohlschlaeger, A., Ille, S., Sollmann, N., Maurer, S., Zimmer, C., Ringel, F., Meyer, B., Krieg, S.M., 2015a. Stimulation frequency determines the distribution of language positive cortical regions during navigated transcranial magnetic brain stimulation. BMC Neurosci. 16 (1), 5. https://doi.org/10.1186/s12868-015-0143-9.

Hauck, T., Tanigawa, N., Probst, M., Wohlschlaeger, A., Ille, S., Sollmann, N., Maurer, S., Zimmer, C., Ringel, F., Meyer, B., Krieg, S.M., 2015b. Task type affects location of language-positive cortical regions by repetitive navigated transcranial magnetic stimulation mapping. PLoS One 10 (4), e0125298. https://doi.org/10.1371/journal.pone.0125298.

Hebart, M.N., Görgen, K., Haynes, J.-D., 2015. The decoding toolbox (TDT): a versatile software package for multivariate analyses of functional imaging data. Front. Neuroinformat. 8. https://www.frontiersin.org/articles/10.3389/fninf.2014.00088.

Heim, S., Alter, K., Ischebeck, A.K., Amunts, K., Eickhoff, S.B., Mohlberg, H., Zilles, K., von Cramon, D.Y., Friederici, A.D., 2005. The role of the left Brodmann's areas 44 and 45 in reading words and pseudowords. Cognit. Brain Res. 25 (3), 982–993. https://doi.org/10.1016/j.cogbrainres.2005.09.022.

Herz, D.M., Christensen, M.S., Bruggemann, N., Hulme, O.J., Ridderinkhof, K.R., Madsen, K.H., Siebner, H.R., 2014. Motivational tuning of fronto-subthalamic connectivity facilitates control of action impulses. J. Neurosci. 34 (9), 3210–3217. https://doi.org/10.1523/JNEUROSCI.4081-13.2014.

Holzer, N., Lenart, F., Schaupp, H., 2017. ERT JE: Eggenberger Rechentest Für Jugendliche und Erwachsene. Hogrefe.

Huang, Y.-Z., Edwards, M.J., Rounis, E., Bhatia, K.P., Rothwell, J.C., 2005. Theta burst stimulation of the human motor cortex. Neuron 45 (2), 201–206. https://doi.org/10.1016/j.neuron.2004.12.033.

Jobard, G., Crivello, F., Tzourio-Mazoyer, N., 2003. Evaluation of the dual route theory of reading: A metanalysis of 35 neuroimaging studies. Neuroimage 20 (2), 693–712. https://doi.org/10.1016/S1053-8119(03)00343-4.

Jung, J.Y., Lambon Ralph, M.A., 2016. Mapping the dynamic network interactions underpinning cognition: a cTBS-fMRI study of the flexible adaptive neural system for semantics. Cereb. Cortex 26 (8), 3580–3590. https://doi.org/10.1093/cercor/bhw149.

Kahan, J., Foltynie, T., 2013. Understanding DCM: Ten simple rules for the clinician. Neuroimage 83, 542–549. https://doi.org/10.1016/j.neuroimage.2013.07.008.

Kersting, M., Althoff, K., 2003. Rechtschreibungstest, 3rd ed. Hogrefe.

Knye, M., Roth, N., Westhus, W., Heine, A., 2003. CPT: Continuous Performance Test, 1st ed. Hogrefe.

Kriegeskorte, N., Goebel, R., Bandettini, P., 2006. Information-based functional brain mapping. Proc. Natl. Acad. Sci. USA. 103 (10), 3863–3868. https://doi.org/10.1073/pnas.0600244103.

Kuhnke, P., Beaupain, M.C., Cheung, V.K.M., Weise, K., Kiefer, M., Hartwigsen, G., 2020a. Left posterior inferior parietal cortex causally supports the retrieval of action knowledge. Neuroimage 219, 117041. https://doi.org/10.1016/j.neuroimage.2020.117041.

Kuhnke, P., Chapman, C.A., Cheung, V.K.M., Turker, S., Graessner, A., Martin, S., Williams, K.A., Hartwigsen, G., 2022. The role of the angular gyrus in semantic cognition: a synthesis of five functional neuroimaging studies. Brain Struct. Funct. https://doi.org/10.1007/s00429-022-02493-y.

Kuhnke, P., Kiefer, M., Hartwigsen, G., 2020b. Task-dependent recruitment of modality-specific and multimodal regions during conceptual processing. Cereb. Cortex 30 (7), 3938–3959. https://doi.org/10.1093/cercor/bhaa010.

Kuhnke, P., Kiefer, M., Hartwigsen, G., 2021. Task-dependent functional and effective connectivity during conceptual processing. Cereb. Cortex 31 (7), 3475–3493. https://doi.org/10.1093/cercor/bhab026.

Lazzaro, G., Costanzo, F., Varuzza, C., Rossi, S., Vicari, S., Menghini, D., 2021. Chapter 8 - effects of a short, intensive, multi-session tDCS treatment in developmental dyslexia: Preliminary results of a sham-controlled randomized clinical trial. In R. C. Kadosh, T. Zaehle, & K. Krauel (Eds.). In: Progress in Brain Research, 264. Elsevier, pp. 191–210. https://doi.org/10.1016/bs.pbr.2021.01.015.

Liederman, J., McGraw Fisher, J., Schulz, M., Maxwell, C., Théoret, H., Pascual-Leone, A, 2003. The role of motion direction selective extrastriate regions in reading: A transcranial magnetic stimulation study. Brain Lang. 85 (1), 140–155. https://doi.org/10.1016/S0093-934X(02)00550-3.

Linkersdörfer, J., Lonnemann, J., Lindberg, S., Hasselhorn, M., Fiebach, C.J., 2012. Grey Matter Alterations Co-Localize with Functional Abnormalities in Developmental Dyslexia: An ALE Meta-Analysis. PLoS One 7 (8), e43122. https://doi.org/10.1371/journal.pone.0043122.

Lo, S., Andrews, S., 2015. To transform or not to transform: Using generalized linear mixed models to analyse reaction time data. Front. Psychol. 6. https://www.frontiersin.org/articles/10.3389/fpsyg.2015.01171.

López-Alonso, V., Cheeran, B., Río-Rodríguez, D., Fernández-del-Olmo, M., 2014. Inter-individual variability in response to non-invasive brain stimulation paradigms. Brain Stimul. 7 (3), 372–380. https://doi.org/10.1016/j.brs.2014.02.004.

Luber, B., Lisanby, H, S., 2014. Enhancement of human cognitive performance using transcranial magnetic stimulation (TMS). Neuroimage 85 (0 3), 961–970. https://doi.org/10.1016/j.neuroimage.2013.06.007.

MacSweeney, M., Brammer, M.J., Waters, D., Goswami, U., 2009. Enhanced activation of the left inferior frontal gyrus in deaf and dyslexic adults during rhyming. Brain 132 (7), 1928–1940. https://doi.org/10.1093/brain/awp129.

Maisog, J.M., Einbinder, E.R., Flowers, D.L., Turkeltaub, P.E., Eden, G.F., 2008. A meta-analysis of functional neuroimaging studies of dyslexia. Ann. N.Y. Acad. Sci. 1145 (1), 237–259. https://doi.org/10.1196/annals.1416.024.

Makris, N., Goldstein, J.M., Kennedy, D., Hodge, S.M., Caviness, V.S., Faraone, S.V., Tsuang, M.T., Seidman, L.J., 2006. Decreased volume of left and total anterior insular lobule in schizophrenia. Schizophr. Res. 83 (2–3), 155–171. https://doi.org/10.1016/j.schres.2005.11.020.

Martin, A., Kronbichler, M., Richlan, F., 2016. Dyslexic brain activation abnormalities in deep and shallow orthographies: a meta-analysis of 28 functional neuroimaging studies. Hum. Brain Mapp. 37 (7), 2676–2699. https://doi.org/10.1002/hbm.23202.

Miniussi, C., Harris, J.A., Ruzzoli, M., 2013. Modelling non-invasive brain stimulation in cognitive neuroscience. Neurosci. Biobehav. Rev. 37 (8), 1702–1712. https://doi.org/10.1016/j.neubiorev.2013.06.014.

Moll, K., Landerl, K., 2010. SLRT-II: Lese- und Rechtschreibtest |, 2nd ed. Hogrefe. https://www.testzentrale.de/shop/lese-und-rechtschreibtest.html#1+1.

Mur, M., Bandettini, P.A., Kriegeskorte, N., 2009. Revealing representational content with pattern-information fMRI—an introductory guide. Soc. Cogn. Affect. Neurosci. 4 (1), 101–109.

Nichols, T. (2023). *SnPM statistical nonparametric mapping: a toolbox for SPM* [Computer software]. http://nisox.org/Software/SnPM13/.

Numssen, O., Bzdok, D., Hartwigsen, G., 2021. Functional specialization within the inferior parietal lobes across cognitive domains. eLife 10, e63591. https://doi.org/10.7554/eLife.63591.

Oberhuber, M., Hope, T.M.H., Seghier, M.L., Parker Jones, O., Prejawa, S., Green, D.W., Price, C.J., 2016. Four functionally distinct regions in the left supramarginal gyrus support word processing. Cereb. Cortex 26 (11), 4212–4226. https://doi.org/10.1093/cercor/bhw251.

Pattamadilok, C., Bulnes, L.C., Devlin, J.T., Bourguignon, M., Morais, J., Goldman, S., Kolinsky, R., 2015. How early does the brain distinguish between regular words, irregular words, and pseudowords during the reading process? evidence from neurochronometric TMS. J. Cogn. Neurosci. 27 (6), 1259–1274. https://doi.org/10.1162/jocn_a_00779.

Peramunage, D., Blumstein, S.E., Myers, E.B., Goldrick, M., Baese-Berk, M., 2011. Phonological Neighborhood Effects in Spoken Word Production: An fMRI Study. J. Cogn. Neurosci. 23 (3), 593–603. https://doi.org/10.1162/jocn.2010.21489.

Power, J.D., Barnes, K.A., Snyder, A.Z., Schlaggar, B.L., Petersen, S.E., 2012. Spurious but systematic correlations in functional connectivity MRI networks arise from subject motion. Neuroimage 59 (3), 2142–2154. https://doi.org/10.1016/j.neuroimage.2011.10.018.

Pugh, K.R., Mencl, W.E., Jenner, A.R., Katz, L., Frost, S.J., Lee, J.R., Shaywitz, S.E., Shaywitz, B.A., 2001. Neurobiological studies of reading and reading disability. J. Commun. Disord. 34 (6), 479–492. https://doi.org/10.1016/S0021-9924(01)00060-0.

Richlan, F., Kronbichler, M., Wimmer, H., 2009. Functional abnormalities in the dyslexic brain: A quantitative meta-analysis of neuroimaging studies. Hum. Brain Mapp. 30 (10), 3299–3308. https://doi.org/10.1002/hbm.20752.

Richlan, F., Kronbichler, M., Wimmer, H., 2011. Meta-analyzing brain dysfunctions in dyslexic children and adults. Neuroimage 56 (3), 1735–1742. https://doi.org/10.1016/j.neuroimage.2011.02.040.

Rueckl, J.G., Paz-Alonso, P.M., Molfese, P.J., Kuo, W.-J., Bick, A., Frost, S.J., Hancock, R., Wu, D.H., Mencl, W.E., Duñabeitia, J.A., Lee, J.-R., Oliver, M., Zevin, J. D., Hoeft, F., Carreiras, M., Tzeng, O.J.L., Pugh, K.R., Frost, R., 2015. Universal brain signature of proficient reading: Evidence from four contrasting languages. Proc. Natl.

Acad. Sci. USA. 112 (50), 15510–15515. https://doi.org/10.1073/pnas.1509321112.

Sale, M.V., Mattingley, J.B., Zalesky, A., Cocchi, L., 2015. Imaging human brain networks to improve the clinical efficacy of non-invasive brain stimulation. Neurosci. Biobehav. Rev. 57, 187–198.

Satterthwaite, T.D., Elliott, M.A., Gerraty, R.T., Ruparel, K., Loughead, J., Calkins, M.E., Eickhoff, S.B., Hakonarson, H., Gur, R.C., Gur, R.E., Wolf, D.H., 2013. An improved framework for confound regression and filtering for control of motion artifact in the preprocessing of resting-state functional connectivity data. Neuroimage 64, 240–256. https://doi.org/10.1016/j.neuroimage.2012.08.052.

Schneider, W., Schlagmüller, Matthias, Ennemoser, Marco., 2017. LGVT 5-12+: Lesegeschwindigkeits- und Verständnistest Für Die Klassen 5–12+. Hogrefe. https://www.testzentrale.de/shop/lesegeschwindigkeits-und-verstaendnistest-fuer-die-klassen-5-12.html#1+1.

Schurz, M., Wimmer, H., Richlan, F., Ludersdorfer, P., Klackl, J., Kronbichler, M., 2015. Resting-state and task-based functional brain connectivity in developmental dyslexia. Cereb. Cortex 25 (10), 3502–3514. https://doi.org/10.1093/cercor/bhu184.

Schuster, S., Hawelka, S., Richlan, F., Ludersdorfer, P., Hutzler, F., 2015. Eyes on words: a fixation-related fMRI study of the left occipito-temporal cortex during self-paced silent reading of words and pseudowords. Sci. Rep. 5 (1) https://doi.org/10.1038/srep12686. Article 1.

Schutter, D.J.L.G., van Honk, J., 2006. A standardized motor threshold estimation procedure for transcranial magnetic stimulation research. J. ECT 22 (3), 176. https://doi.org/10.1097/01.yct.0000235924.60364.27.

Seghier, M.L., 2023. Multiple functions of the angular gyrus at high temporal resolution. Brain Struct. Funct. 228 (1), 7–46. https://doi.org/10.1007/s00429-022-02512-y.

Seidenberg, M.S., 2005. Connectionist models of word reading. Curr. Dir. Psychol. Sci. 14 (5), 238–242. https://doi.org/10.1111/j.0963-7214.2005.00372.x.

Siebner, H., Rothwell, J., 2003. Transcranial magnetic stimulation: new insights into representational cortical plasticity. Exp. Brain Res. 148 (1), 1–16. https://doi.org/10.1007/s00221-002-1234-2.

Siegel, J.S., Power, J.D., Dubis, J.W., Vogel, A.C., Church, J.A., Schlaggar, B.L., Petersen, S.E., 2014. Statistical improvements in functional magnetic resonance imaging analyses produced by censoring high-motion data points. Hum. Brain Mapp. 35 (5), 1981–1996. https://doi.org/10.1002/hbm.22307.

Smallwood, J., Bernhardt, B.C., Leech, R., Bzdok, D., Jefferies, E., Margulies, D.S., 2021. The default mode network in cognition: a topographical perspective. Nat. Rev. Neurosci. 22 (8), 503–513.

Stoodley, C.J., Schmahmann, J.D., 2009. Functional topography in the human cerebellum: a meta-analysis of neuroimaging studies. Neuroimage 44 (2), 489–501. https://doi.org/10.1016/j.neuroimage.2008.08.039.

Taylor, J.S.H., Rastle, K., Davis, M.H., 2013. Can cognitive models explain brain activation during word and pseudoword reading? A meta-analysis of 36 neuroimaging studies. Psychol. Bull. 139 (4), 766–791. https://doi.org/10.1037/a0030266.

Tops, M., Boksem, M., 2011. A potential role of the inferior frontal gyrus and anterior insula in cognitive control, brain rhythms, and event-related potentials. Front. Psychol. 2. https://www.frontiersin.org/articles/10.3389/fpsyg.2011.00330.

Turker, S., 2018. Exploring the neurofunctional underpinnings of developmental dyslexia: a review focusing on dyslexic children. In: Marin, M., Luef, E. (Eds.), The Talking Species: Perspectives on the Evolutionary, Neuronal and Cultural Foundations of Language. Unipress, pp. 337–377.

Turker, S., Hartwigsen, G., 2021. Exploring the neurobiology of reading through non-invasive brain stimulation: a review. Cortex 141, 497–521. https://doi.org/10.1016/j.cortex.2021.05.001.

Turker, S., Hartwigsen, G., 2022. The use of noninvasive brain stimulation techniques to improve reading difficulties in dyslexia: a systematic review. Hum. Brain Mapp. 43 (3), 1157–1173. https://doi.org/10.1002/hbm.25700.

Turker, S., Kuhnke, P., 2023. Adaptive Short-Term Plasticity in the Typical Reading Network. osf.io/fpgcy.

Turker, S., Kuhnke, P., Eickhoff, S., Caspers, S., Hartwigsen, G., 2023. Cortical, subcortical and cerebellar contributions to language processing: A meta-analytic review of 403 neuroimaging experiments. Psychol. Bull.

Valdois, S., Lassus-Sangosse, D., Lallier, M., Moreaud, O., Pisella, L., 2019. What bilateral damage of the superior parietal lobes tells us about visual attention disorders in developmental dyslexia. Neuropsychologia 130, 78–91. https://doi.org/10.1016/j.neuropsychologia.2018.08.001.

van der Mark, S., Klaver, P., Bucher, K., Maurer, U., Schulz, E., Brem, S., Martin, E., Brandeis, D., 2011. The left occipitotemporal system in reading: Disruption of focal fMRI connectivity to left inferior frontal and inferior parietal language areas in children with dyslexia. Neuroimage 54 (3), 2426–2436. https://doi.org/10.1016/j.neuroimage.2010.10.002.

Wang, Q., Akram, H., Muthuraman, M., Gonzalez-Escamilla, G., Sheth, S.A., Oxenford, S., Yeh, F.-C., Groppa, S., Vanegas-Arroyave, N., Zrinzo, L., Li, N., Kühn, A., Horn, A., 2021. Normative vs. Patient-specific brain connectivity in deep brain stimulation. Neuroimage 224, 117307. https://doi.org/10.1016/j.neuroimage.2020.117307.

Wechsler, D., 2008. WAIS - IV - Wechsler Adult Intelligence Scale, 4th ed. Pearson https://www.pearsonclinical.de/wais-iv.html.

Weiß, R.H., 2019. CFT 20-R: Grundintelligenztest Skala 2—Revision. Hogrefe.

Xia, Z., Zhang, L., Hoeft, F., Gu, B., Gong, G., Shu, H., 2018. Neural correlates of oral word reading, silent reading comprehension, and cognitive subcomponents. Int. J. Behav. Dev. 42 (3), 342–356. https://doi.org/10.1177/0165025417727872.

Zeidman, P., Jafarian, A., Corbin, N., Seghier, M.L., Razi, A., Price, C.J., Friston, K.J., 2019a. A guide to group effective connectivity analysis, part 1: first level analysis with DCM for fMRI. Neuroimage 200, 174–190. https://doi.org/10.1016/j.neuroimage.2019.06.031.

Zeidman, P., Jafarian, A., Seghier, M.L., Litvak, V., Cagnan, H., Price, C.J., Friston, K.J., 2019b. A guide to group effective connectivity analysis, part 2: second level analysis with PEB. Neuroimage 200, 12–25. https://doi.org/10.1016/j.neuroimage.2019.06.032.